#3

NEW METHOD OF MEASURING THE NOISE PARAMETERS OF THE ELECTRON BEAM, ESPECIALLY THE CORRELATION BETWEEN ITS VELOCITY AND CURRENT FLUCTUATIONS

SHIGEBUMI SAITO

TECHNICAL REPORT 333

AUGUST 22, 1957

RESEARCH LABORATORY OF ELECTRONICS
MASSACHUSETTS INSTITUTE OF TECHNOLOGY
CAMBRIDGE, MASSACHUSETTS

The Research Laboratory of Electronics is an interdepartmental laboratory of the Department of Electrical Engineering and the Department of Physics.

The research reported in this document was made possible in part by support extended the Massachusetts Institute of Technology, Research Laboratory of Electronics, jointly by the U. S. Army (Signal Corps), the U. S. Navy (Office of Naval Research), and the U. S. Air Force (Office of Scientific Research, Air Research and Development Command), under Signal Corps Contract DA36-039-sc-64637, Department of the Army Task 3-99-06-108 and Project 3-99-00-100.

MASSACHUSETTS INSTITUTE OF TECHNOLOGY

RESEARCH LABORATORY OF ELECTRONICS

Technical Report 333 August 22, 1957

NEW METHOD OF MEASURING THE NOISE PARAMETERS OF THE ELECTRON BEAM, ESPECIALLY THE CORRELATION BETWEEN ITS VELOCITY AND CURRENT FLUCTUATIONS

Shigebumi Saito

Abstract

The noise figure of a microwave beam amplifier has a lower limit that depends entirely upon the noise process in the electron gun at and near the potential minimum. This report is chiefly concerned with the theory and experimental results of a new method of measuring the noise parameters of the electron beam, especially the correlation between its velocity and current fluctuations, by using a selective beam coupler that has properties similar to the conventional microwave directional coupler. The value of the correlation coefficient of the velocity and current fluctuations was found to be from 0.2 to 0.35 in the space-charge-limited region and zero, or slightly negative, in the temperature-limited region. The probable error of this measuring method is discussed by taking account of the residual selectivity of the selective beam coupler, the effect of the pickup cavities upon the beam, the thermal noise from these cavities, and the higher-order modes.

I. INTRODUCTION

From recent theoretical work the conclusion can be drawn that the noise figure of a microwave beam amplifier has a lower limit that depends entirely upon the noise process in the electron gun at and around the potential minimum (1, 2, 3, 4). No exact theoretical solution for the noise process at the potential minimum is now available. Therefore, the exact value of the critical noise parameter that determines the lower limit of the noise figure is unknown.

All of the present theories have been based on plausible assumptions, which, nevertheless, raise the question of their applicability to practical cases. The present paper is concerned with a method of measurement that yields independent sets of data for the critical noise parameter, and will thus provide not only checkpoints for the accuracy of the measurement, but also give an indication of the validity of the theory.

In the notation of Haus and Robinson (3), the lower limit of the noise figure of a microwave beam amplifier is given by

$$F_{min} = 1 + \frac{2\pi}{kT}(1 - 1/G)(S-\Pi) \tag{1}$$

where T is the temperature of the circuit, G is the available gain of the amplifier, and (S-Π) is the critical noise parameter determined entirely by the noise process at the potential minimum. Both S and Π are independently measurable. The value of S is given by a measurement of the noise-current standing wave in a drift tube as

$$4\pi\,\Delta f\,S^2 = Y_o^2\,|\overline{i_{max}}|^2\,|\overline{i_{min}}|^2 \tag{2}$$

where $|\overline{i_{max}}|^2$ and $|\overline{i_{min}}|^2$ are the mean-square amplitudes of the noise current in the electron beam within the frequency band Δf at the maximum and minimum of the standing wave, respectively. Y_o is the characteristic admittance of the beam,

$$Y_o = \frac{I_o}{2V_o}\frac{\lambda_q}{\lambda_e} \tag{3}$$

where I_o and V_o are the time-average current and voltage of the electron beam in the drift region, λ_q is the reduced plasma wavelength, and λ_e is the electronic wavelength. All the quantities on the right-hand side of Eq. 2 are either measurable or derivable from measured quantities. Thus, for example, a standing-wave measurement by means of a cavity that slides along the electron beam and registers the noise current in the electron beam can yield a value of S (5, 6, 7) through Eq. 2. The quantity Π is much harder to measure. Two methods for the measurement of the ratio Π/S have been devised and preliminary measurements based on them have been made (7, 8). In both of these methods the determination of Π/S involves a knowledge of S. This paper is chiefly concerned with the measurement of the ratio Π/S independently of S. If we

combine the measurement of Π/S with a measurement of S, the critical noise parameter $S - \Pi$ can be found.

The selective beam coupler devised for the measurement of Π/S picks up either the noise carried in the fast-beam wave, or the noise in the slow wave. The value of Π/S can be derived from the ratio of two outputs of the selective beam coupler.

II. PRINCIPLE OF THE SELECTIVE BEAM COUPLER

In terms of the normalized amplitudes a_1 and a_2 of the fast and slow waves in an electron beam, the rf kinetic voltage and rf current in the electron beam can be written as (3)

$$V = \sqrt{2Z_o}\left(a_1 e^{j\beta_q z} - a_2 e^{-j\beta_q z}\right) e^{-j\beta_e z}$$
$$i = \sqrt{2Y_o}\left(a_1 e^{j\beta_q z} + a_2 e^{-j\beta_q z}\right) e^{-j\beta_e z} \tag{4}$$

where β_q is the reduced plasma propagation constant, β_e is the electronic propagation constant, $\beta_e = \omega/v_o$ and $Y_o = 1/Z_o$ is the characteristic admittance of the beam.

The selective coupler consists of two cavities, separated by a distance Δz, as shown in Fig. 1. The noise current picked up by the second cavity comes partly from the noise in the beam in the absence of the first cavity, and partly from a twofold effect of the first cavity: The first cavity affects the fields in the beam by its mere presence, and the thermal noise in the first cavity produces a voltage across its gap and modulates the electron beam. If we neglect the thermal-noise voltage produced across the gap of the first cavity, we can represent the effect of the first cavity (provided its gap is sufficiently short) as a series impedance in the equivalent transmission line of the electron beam, as shown in Fig. 2. Let I_1 and I_2 be the output currents of cavities 1 and 2. (Hereafter, it is assumed that both cavities are identical; the general case is treated in Appendix I.) These output currents are related to the beam current by a proportionality constant K.

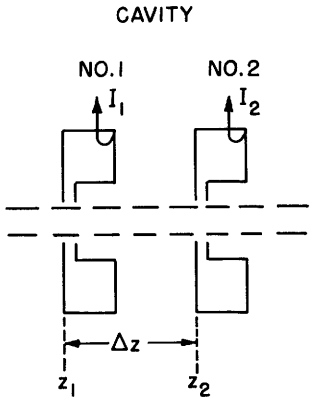

Fig. 1. Two pickup cavities separated by distance Δz.

$$I_1 = K\left(a_1 e^{j\beta_q z_1} + a_2 e^{-j\beta_q z_1}\right) e^{-j\beta_e z_1}$$
$$I_2 = K\left\{a_1 e^{j\beta_q z_1}\left(e^{j\beta_q \Delta z} - jZ \sin \beta_q \Delta z\right)\right. \tag{5}$$
$$\left. + a_2 e^{-j\beta_q z_1}\left(e^{-j\beta_q \Delta z} - jZ \sin \beta_q \Delta z\right)\right\} e^{-j\beta_e (z_1 + \Delta z)}$$

where Z is the gap shunt impedance of the first cavity normalized with respect to the

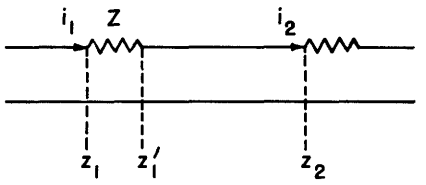

Fig. 2. Equivalent circuit of the pickup cavities, as seen from the beam.

beam impedance; we assume that $Z < 1$, because this choice of Z is convenient for several reasons which will be discussed later.

The currents of cavities 1 and 2 are added in a hybrid Tee junction. Phase-shifters and attenuators placed in the output lines of cavities 1 and 2 introduce phase shifts, $-\psi_1$ and ψ_2, and losses, L_1 and L_2. The sum of the two output currents can be given, if we neglect the total phase shift $-\psi_T$ by

$$I_t = L_1 I_1 e^{-j\psi} + L_2 I_2 \tag{6}$$

where $\psi = \psi_1 - \psi_2$. For case a: for the total current I_{ta}, we obtain

$$I_{ta} = K e^{-j\psi_a} \left[a_1 e^{-j\beta_q z_1} \{L_1 - (1-Z) L_2\} + a_2 e^{-j\beta_q z_1} \{L_1 + (1+Z) L_2\} \right] e^{-j\beta_e z_1} \tag{7}$$

With a proper adjustment of the loss in the attenuators, $L_{1a} = (1-Z) L_{2a}$, we have

$$I_{ta} = K L_{2a} e^{-j\psi_a} 2a_2 e^{-j(\beta_e+\beta_q)z_1} \tag{8}$$

Similarly, for case b: with the choice $L_{1b} = (1+Z) L_{2b}$, we obtain

$$I_{tb} = K L_{2b} e^{-j\psi_b} 2a_1 e^{-j(\beta_e-\beta_q)z_1} \tag{9}$$

In actual measurements, it can be taken that $L_{2a} = 1.0$ and $L_{1b} = 1.0$, and therefore $L_{1a} = 1 - Z$ and $L_{2b} = 1/1 + Z$. Since it is assumed here that $Z < 1$, L_{1a} and L_{2b} are less than unity and thus they signify attenuation.

Equations 8 and 9 show that in case a it is possible to pick up only the slow-wave component of the beam current, and only the fast-wave component in case b. This is the principle of operation of the conventional microwave directional coupler. Our device resembles such a coupler. When the value of Z is known (a method of obtaining it will be described later), we can obtain the ratio $|a_2|^2/|a_1|^2$ directly from the measured value of $|I_{ta}|^2/|I_{tb}|^2$.

We denote by a_1 and a_2 the normalized amplitudes of the fast and slow waves of the beam noise. The values of the noise quantities S and Π are related to averages of a_1 and a_2 as follows:

$$S = \frac{1}{4\pi} \left\{ \left[|\overline{a_1}|^2 + |\overline{a_2}|^2 \right]^2 - 4 |\overline{a_1 a_2^*}|^2 \right\}^{1/2} \tag{10}$$

$$\Pi = \frac{1}{4\pi} \left\{ |\overline{a_1}|^2 - |\overline{a_2}|^2 \right\} \tag{11}$$

The bars denote ensemble averages and the stars denote complex-conjugate values. The ratio of the maximum to the minimum of the mean-square beam current ρ^2 is given by

$$\rho^2 = \frac{1 + |\overline{a_2}|^2/|\overline{a_1}|^2 + 2|\overline{a_1 a_2^*}|/|\overline{a_1}|^2}{1 + |\overline{a_2}|^2/|\overline{a_1}|^2 - 2|\overline{a_1 a_2^*}|/|\overline{a_1}|^2} \tag{12}$$

Hence

$$\frac{\Pi}{S} = \frac{1}{2\rho/(1+\rho^2)} \frac{1 - |\overline{a_2}|^2/|\overline{a_1}|^2}{1 + |\overline{a_2}|^2/|\overline{a_1}|^2} \tag{13}$$

The ratio $|\overline{a_2}|^2/|\overline{a_1}|^2$ is known from the measured value of $|\overline{I_{ta}}|^2/|\overline{I_{tb}}|^2$, as before. Therefore Π/S can be obtained independently of the absolute value of S, once the value ρ^2 is known.

The value of ρ^2 can be determined as follows. The two cavities are separated by the distance $\Delta z = \pi/\beta_q$ ($= \lambda_q/2$, where λ_q is the plasma wavelength of the beam). Furthermore, ψ is adjusted to the value $\psi_c = \pi + \beta_e \Delta z$. The following equation is easily obtained from Eqs. 5 and 6.

$$I_{tc} = L_c I_1 e^{-j\psi_c} + I_2 = K e^{-j\psi_c}(1 + L_c)\left\{a_1 e^{-j\beta_q z_1} + a_2 e^{-j\beta_q z_1}\right\} e^{-j\beta_e z_1} \tag{14}$$

It should be noted that Eq. 16 does not contain the impedance of the first cavity. This is an indication that the presence of the first cavity has no effect upon the measurement. When we move both cavities together along the beam, a periodical variation of $|I_{tc}|^2$ is obtained. The ratio of the maximum to the minimum of $|I_{tc}|^2$ gives the value of ρ^2.

According to Eqs. 8 and 9, the selectivity of the selective beam coupler is infinite. In practice, the selectivity will be finite, if the adjustment of the coupler is faulty, or, as will be seen later, because of the finite bandwidth of the pickup cavities. We shall now discuss a method of eliminating the effect of a finite selectivity of the coupler.

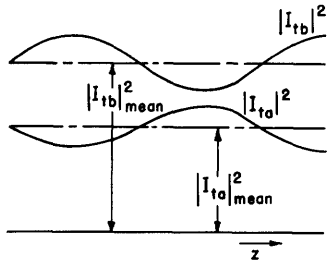

Fig. 3. Standing-wave patterns of output currents, $|I_{ta}|^2$ and $|I_{tb}|^2$, along the beam.

We denote by α_a the fractional response of the selective coupler to the fast wave in case a (in which the coupler should respond to the slow wave). In case b the coupler should respond only to the fast wave. We denote by α_b the fractional response to the slow wave. Then the total currents I_{ta} and I_{tb} can

be expressed as (see Fig. 3)

$$\left.\begin{aligned} |I_{ta}|^2 &= K_1^2 \left\{ |\alpha_a|^2 \, |a_1|^2 + |a_2|^2 + 2|\alpha_a| \, |a_1 a_2^*| \cos(2\beta_q z_1 - \phi_1) \right\} \\ |I_{tb}|^2 &= K_2^2 \left\{ |a_1|^2 + |\alpha_b|^2 \, |a_2|^2 + 2|\alpha_b| \, |a_1 a_2^*| \cos(2\beta_q z_1 - \phi_2) \right\} \end{aligned}\right\} \tag{15}$$

Since α is usually much less than 1, α^2 is negligibly small; nevertheless α may be important. In order to eliminate the effect of the residual lack of selectivity, we do not record I_{ta} and I_{tb} at single positions of the cavities. Instead, we move both cavities along the beam. Equation 15 shows that an average of the readings taken over one-half of a space-charge wavelength will eliminate the contributions to I_{ta} and I_{tb} covered by the residual lack of selectivity. These average values of $|I_{ta}|^2$ and $|I_{tb}|^2$ are given by

$$\begin{aligned} |I_{ta}|^2_{mean} &= K_1^2 \left\{ |\alpha_a|^2 \, |a_1|^2 + |a_2|^2 \right\} \\ |I_{tb}|^2_{mean} &= K_2^2 \left\{ |a_1|^2 + |\alpha_b|^2 \, |a_2|^2 \right\} \end{aligned} \tag{16}$$

Since $|\alpha_a|^2$ and $|\alpha_b|^2$ are very small, Eqs. 16 give an accurate indication of the wave amplitudes.

III. CHARACTERISTICS OF SELECTIVE BEAM COUPLER

3.1 FREQUENCY CHARACTERISTICS OF THE SELECTIVE BEAM COUPLER

Our investigation thus far has been confined to measurements over a very small frequency band, so that the frequency dependence of the cavity impedances can be neglected. We shall now derive the general characteristics of the selective beam coupler by taking into account the frequency dependence of the cavity impedances. The equivalent circuit of the selective beam coupler is shown in Fig. 4. We assume, as before, that cavities 1 and 2 are identical, because this case is the most important.

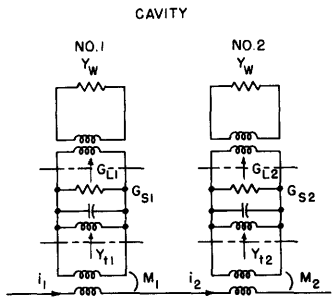

Fig. 4. Equivalent circuit of the two pick-up cavities, with all of the circuit parameters taken into account.

The output current I is related to the beam current i at the cavity gap

$$I = M\left(\frac{G_L}{Y_t}\right)i \tag{17}$$

where G_L and Y_t are the load conductance and total admittance of the cavity, as seen at the gap, and M is the gap-coupling coefficient. The frequency dependence of the cavity admittance Y_t in the vicinity of resonance is given by

$$Y_t = G_t(1 + jx)$$
$$x = 2Q_L \frac{\omega - \omega_o}{\omega_o} \tag{18}$$

where G_t is the total conductance of the cavity, Q_L is the loaded Q of the cavity, ω is the variable angular frequency, and ω_o is the resonant angular frequency of the cavity.

The normalized series impedance Z that expresses the effect of the first cavity upon the beam is given by

$$Z = M^2\left(\frac{Y_o}{Y_t}\right) = \frac{r}{1 + jx} \tag{19}$$

where $r(= Y_o M^2/G_t)$ is the normalized resistance of the cavities, as seen from the beam, at the resonant frequency of the cavity.

By using Eqs. 17, 18, and 19, the general output currents I_{ta} and I_{tb}, corresponding to Eqs. 8 and 9, can be obtained.

For case a: $\beta_q \Delta z = \pi/2$, $\psi_a = \pi/2 + \beta_e \Delta z$. With the choice of $L_{1a} = (1-r)\, L_{2a}$, we have

$$I_{ta} = \sqrt{2Y_o}(ML_{2a})\left(\frac{G_L}{G_t}\right)\frac{1}{1+jx}\, e^{-j\psi_a}\left\{\left(\frac{-jx}{1+jx}\, r\right) a_1\, e^{j\beta_q z_1}\right.$$

$$\left. + \left(2 - \frac{jxr}{1+jx}\right) a_2\, e^{-j\beta_q z_1}\right\} e^{-j\beta_e z_1} \tag{20}$$

For case b: $\beta_q \Delta z = \pi/2$, $\psi_b = -\pi/2 + \beta_e \Delta z$. With the choice of $L_{1b} = (1+r)L_{2b}$, we have

$$I_{tb} = \sqrt{2Y_o}(ML_{2b})\left(\frac{G_L}{G_t}\right)\frac{1}{1+jx}\, e^{-j\psi_b}\left\{\left(2 + \frac{jxr}{1+jx}\right) a_1\, e^{j\beta_q z_1}\right.$$

$$\left. + \left(\frac{jxr}{1+jx}\right) a_2\, e^{-j\beta_q z_1}\right\} e^{-j\beta_e z_1} \tag{21}$$

Note that at $x = 0$ (at resonance of both cavities), Eqs. 20 and 21 reduce to Eqs. 8 and 9, respectively. The selectivity of the selective coupler is infinite at resonance, but off resonance the selectivity becomes finite because of the frequency dependence of the cavity impedances.

In order to obtain good sensitivity, we have to measure the noise output of the cavities over as large a frequency band as possible, i.e., the bandwidth of the cavity. Thus, the measuring device integrates the square of Eqs. 2 and 21 over the cavity bandwidth. Assuming that the detector bandwidth is wide compared with the cavity bandwidth (the effect of the finite bandwidth of the detector is discussed in Appendix III), we obtain directly

$$\left.\begin{aligned}
\sum |I_{ta}|^2 &= \int_{-\infty}^{\infty} |I_{ta}|^2\, dx = C_1\left\{\frac{r^2}{8} A_1 + \left(1 - \frac{r}{2} + \frac{r^2}{8}\right) A_2 - \frac{r}{2}\left(1 - \frac{r}{2}\right) A_{12}\right. \\
&\qquad \left.\times \cos(2\beta_q z_1 + \xi)\right\} \\
\sum |I_{tb}|^2 &= \int_{-\infty}^{\infty} |I_{tb}|^2\, dx = C_2\left\{\left(1 + \frac{r}{2} + \frac{r^2}{8}\right) A_1 + \frac{r^2}{8} + A_2 + \frac{r}{2}\left(1 + \frac{r}{2}\right) A_{12}\right. \\
&\qquad \left.\times \cos(2\beta_q z_1 + \xi)\right\} \\
C_{\substack{1,\\2}} &= 32\pi^2 (ML_{\substack{2a,\\2b}})^2 \left(\frac{G_L}{G_t}\right)^2 Y_o
\end{aligned}\right\} \tag{22}$$

where r is the normalized series resistance at the resonant frequency of both cavities, and hence expresses the effect of the first cavity upon the beam, and A_1, A_2, and A_{12}

are the parameters defined by Haus and Robinson (3). The relations among the a's and A's can be expressed as

$$\left.\begin{aligned} A_1 &= \frac{|a_1|^2}{4\pi}, & A_2 &= \frac{|a_2|^2}{4\pi}, \\ A_{12} &= \frac{|a_1 a_2^*|}{4\pi}, & \xi &= \arg A_{12}, \\ \Pi &= A_2 - A_1 \\ S &= \left\{(A_1 + A_2)^2 - 4A_{12}A_{12}^*\right\}^{1/2} \end{aligned}\right\} \tag{23}$$

If we take the average values of Eq. 23, then we obtain

$$\left.\begin{aligned} \sum |I_{ta}|^2_{mean} &= C_1\left(1 - \frac{r}{2} + \frac{r^2}{8}\right)\left\{\frac{r^2}{8}\,\frac{1}{1 - \frac{r}{2} + \frac{r^2}{8}}\,A_1 + A_2\right\} \\ \sum |I_{tb}|^2_{mean} &= C_2\left(1 + \frac{r}{2} + \frac{r^2}{8}\right)\left\{A_1 + \frac{r^2}{8}\,\frac{1}{1 + \frac{r}{2} + \frac{r^2}{8}}\,A_2\right\} \end{aligned}\right\} \tag{24}$$

By comparing Eqs. 24 with Eqs. 15, we can see that the selectivities which are finite, as expected from Eqs. 20 and 21, are given by

$$\left.\begin{aligned} 10\log_{10}|a_a|^2 &= 10\log_{10}\frac{r^2}{8\left(1 - \frac{r}{2} + \frac{r^2}{8}\right)} \\ 10\log_{10}|a_a|^2 &= 10\log_{10}\frac{r^2}{8\left(1 + \frac{r}{2} + \frac{r^2}{8}\right)} \end{aligned}\right\} \tag{25}$$

The selectivity of the selective beam coupler deteriorates as the real part of the normalized series impedance, r, produced by the first cavity, increases. Therefore r must be kept reasonably small ($r < 1$).

In our discussion we have neglected the frequency dependence of the propagation constant of the electron beam $\beta_e(=\omega/v_o)$, because the Q's of the pickup cavities are usually so high that the frequency dependence of β_e is negligibly small compared with that of the cavity impedances.

3.2 THERMAL NOISE FROM THE CAVITY

Thus far we have neglected the thermal noise from cavities 1 and 2. Thermal noise from cavity 1 is troublesome, because a part of it is transmitted by the electron beam.

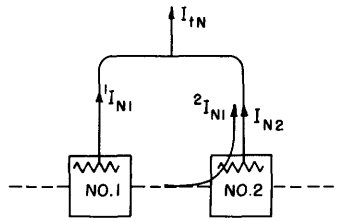

Fig. 5. Thermal-noise currents from the pickup cavities.

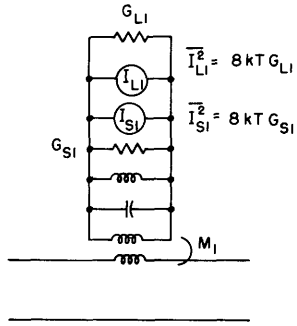

Fig. 6. Equivalent circuit for thermal noise from the first cavity.

This component of the thermal noise is correlated at the Tee junction with the noise coming directly from cavity 1. A correlation of this kind can give rise to a false reading.

The following sources of thermal noise must be distinguished (see Fig. 5).

The noise current I_{N1}^1: from the thermal noise of cavity 1, at its output.

The noise current I_{N1}^2: from the thermal noise of cavity 1, transmitted by the beam and passed through the output line of cavity 2.

The noise current I_{N2}: from the thermal noise of cavity 2.

Then, the total noise current I_{tN} can be given as

$$I_{tN} = I_{N1}^1 e^{j\theta_1} + I_{N1}^2 e^{j\theta_2} + I_{N2} e^{j\theta_3} \tag{26}$$

where, θ_1, θ_2, and θ_3 are phase angles of I_{N1}^1, I_{N1}^2, and I_{N2}, respectively. Since the noise currents I_{N1}^1 and I_{N1}^2 from cavity 1 are perfectly correlated, and I_{N2} is not correlated with the other currents, the following equation can be obtained:

$$|\overline{I_{tN}}|^2 = |\overline{I_{No}^1}|^2 + |\overline{I_{N1}^2}|^2 + 2|I_{No}^1 I_{N1}^2| \cos(\theta_1 - \theta_2) + |I_{N2}|^2 \tag{27}$$

where the first and last terms indicate the thermal-noise currents that exist even when the electron beam is absent. These two terms are balanced out by the receiving radiometer (6, 7).

We shall now calculate the second and third terms of Eq. 27. The equivalent circuit of the noise sources of cavity 1 is shown in Fig. 6.

$$|\overline{I_{N1}^2}|^2 = (ML_{2a})^2 \left(\frac{G_L}{G_t}\right)^2 Y_o \frac{r}{(1+x^2)^2} 8\,kT \tag{28}$$

For case a: ($\beta_q \Delta z = \pi/2$, $\psi_a = \pi/2 + \beta_e \Delta z$ and $L_{1a} = (1-r)L_{2a}$)

$$2|I_{N1}^1 I_{N1}^{2*}| \cos(\theta_1 - \theta_2) = -2(ML_{2a})^2 \left(\frac{G_L}{G_t}\right)^2 Y_o \frac{1-r}{(1+x^2)^2} 8\,kT \tag{29}$$

For case b: ($\beta_q \Delta z = \pi/2$, $\psi_b = -\pi/2 + \beta_e \Delta z$ and $L_{2b} = (1+r) L_{2a}$)

$$2\left|I_{N1}^{1} I_{N1}^{2}\right| \cos(\theta_1 - \theta_2) = 2 (ML_{2b})^2 \left(\frac{G_L}{G_t}\right)^2 Y_o \frac{1 + r}{(1 + x^2)^2} 8\,kT \tag{30}$$

After integrating the noise terms $\left|I_{N1}^{2}\right|^2$ and $2\left|I_{N1}^{1} I_{N1}^{2*}\right| \cos(\theta_1 - \theta_2)$ from minus infinity to plus infinity with respect to x, we add them to Eq. 24, and then the final equations for $\Sigma \left|I_{ta}\right|^2_{mean}$ and $\Sigma \left|I_{tb}\right|^2_{mean}$ are obtained:

$$\left.\begin{aligned}
\sum \left|I_{ta}\right|^2_{mean} &= C_1 \left(1 - \frac{r}{2} + \frac{r^2}{8}\right)\left\{\frac{r^2}{8} \frac{1}{1 - \frac{r}{2} + \frac{r^2}{8}} A_1 + A_2 \right. \\
&\qquad \left. - \frac{1}{2} \frac{1 - \frac{3}{2} r}{1 - \frac{r}{2} + \frac{r^2}{8}} \left(\frac{kT}{2\pi}\right)\right\} \\
\sum \left|I_{tb}\right|^2_{mean} &= C_2 \left(1 + \frac{r}{2} + \frac{r^2}{8}\right)\left\{A_1 + \frac{r}{8} \frac{1}{1 + \frac{r}{2} + \frac{r^2}{8}} A_2 \right. \\
&\qquad \left. + \frac{1}{2} \frac{1 + \frac{3}{2} r}{1 + \frac{r}{2} + \frac{r^2}{8}} \left(\frac{kT}{2\pi}\right)\right\}
\end{aligned}\right\} \tag{31}$$

The last terms of Eqs. 31 indicate the effect of the thermal noise from the first cavity upon the output currents. It should be noted that the factor preceding $(kT/2\pi)$ is of the same order of magnitude as the factor preceding A_2, for case a, or A_1, for case b, with the assumption that $r \ll 1$. In other words, the effect of the thermal noise does not vary appreciably, whether the cavities are tightly coupled with the beam (r is reasonably large), or loosely coupled (r is small). But the selectivity of the selective coupler decreases in proportion to r.

Substituting $\Pi = A_1 - A_2$ in Eq. 31, we obtain

$$\left(\frac{A_2}{A_1}\right)_{apparent} = \frac{K_2 \Sigma \left|I_{ta}\right|^2_{mean}}{K_1 \Sigma \left|I_{tb}\right|^2_{mean}} = \left(\frac{A_2}{A_1}\right)_{true} \frac{1 + \frac{r^2}{8\left(1 - \frac{r}{2} + \frac{r^2}{8}\right)}\left(\frac{A_1}{A_2}\right) - \frac{\left(1 - \frac{3}{2} r\right)}{2\left(1 - \frac{r}{2} + \frac{r^2}{8}\right)}\left(\frac{A_1}{A_2} - 1\right)\frac{\left(\frac{kT}{2\pi}\right)}{\Pi}}{1 + \frac{r^2}{8\left(1 + \frac{r}{2} + \frac{r^2}{8}\right)}\left(\frac{A_2}{A_1}\right) + \frac{\left(1 + \frac{3}{2} r\right)}{2\left(1 + \frac{r}{8} + \frac{r^2}{8}\right)}\left(1 - \frac{A_2}{A_1}\right)\frac{\left(\frac{kT}{2\pi}\right)}{\Pi}} \tag{32}$$

where K_2/K_1 is given as

$$\frac{K_2}{K_1} = \left(\frac{L_{2b}}{L_{2a}}\right)^2 \frac{1 + \frac{r}{2} + \frac{r^2}{8}}{1 - \frac{r}{2} + \frac{r^2}{8}}$$

and, from actual measurements, we have $\left(\frac{L_{2b}}{L_{2a}}\right)^2 = \frac{1}{(1+r)^2}$. Since all the quantities on the right-hand side of Eq. 32 are either measurable or derivable from measured quantities, we can compute the true value of $\frac{A_2}{A_1}$. Usually, this compensation term is small, less than 15 per cent, as shown in Section VI.

Although Eq. 31 is a solution for the special case in which the two cavities are identical and the bandwidth of the detector circuit is wide compared with cavity bandwidth, it can be shown (Appendix I, II, III) that in the more general case

$$\sum |I_{ta}|^2_{mean} = K_1\left\{|\alpha_a|^2 A_1 + A_2 - \beta_a\left(\frac{kT}{2\pi}\right)\right\}$$

$$\sum |I_{tb}|^2_{mean} = K_2\left\{A_2 + |\alpha_b|^2 A_2 + \beta_b\left(\frac{kT}{2\pi}\right)\right\} \qquad (33)$$

where $|\alpha_a|$ and $|\alpha_b|$ are the inverses of the selectivity of the selective beam coupler because of the frequency dependences of the cavity impedances and the finite bandwidth of the detector circuit, and β_a and β_b are the factors that show the effect of the thermal noise from the first cavity.

In the measurements of S, in which the two cavities are one-half of a plasma wavelength apart, the thermal noise from the first cavity does not affect the measurement.

IV. MEASURING EQUIPMENT

The diagram of the measuring equipment is illustrated in Fig. 7. Two movable cavities were designed to have a sufficiently high $R_s M^2/Q$ (where R_s is the shunt resistance of the cavity at the gap, Q_o is the unloaded Q of the cavity, and M is the product of geometric and transit-time beam-coupling coefficients). The amount of noise picked up by the cavities is directly proportional to this factor. The two cavities were adjusted so that they had approximately the characteristics shown in Table I. These cavities were movable along the electron beam over a distance of approximately 20 cm.

The outputs of the pickup cavities were added in the Magic Tee after the appropriate phase shifts and attenuations that are required by the theory of measurement. The output of the H-branch of the Magic Tee was fed to the radiometer. In this device the noise power is modulated at 30 cps before it enters the microwave receiver. The output of the receiver was then fed to a 30-cps lock-in amplifier in which the modulated noise was synchronously detected.

The microwave receiver consisted of a balanced mixer that feeds a 30-mc low-noise i-f amplifier with a bandwidth of 6.5 mc. The operating noise figure of the receiver was 9.5 db. The ferrite isolator at the input of the receiver was used to prevent any reflected local-oscillator power from being modulated at 30 cps.

During all the measurements, the output of the radiometer was kept at ten times the value of the inherent fluctuations of the measuring system. By using this procedure for estimating the sensitivity of the radiometer, it was found that a noise power of

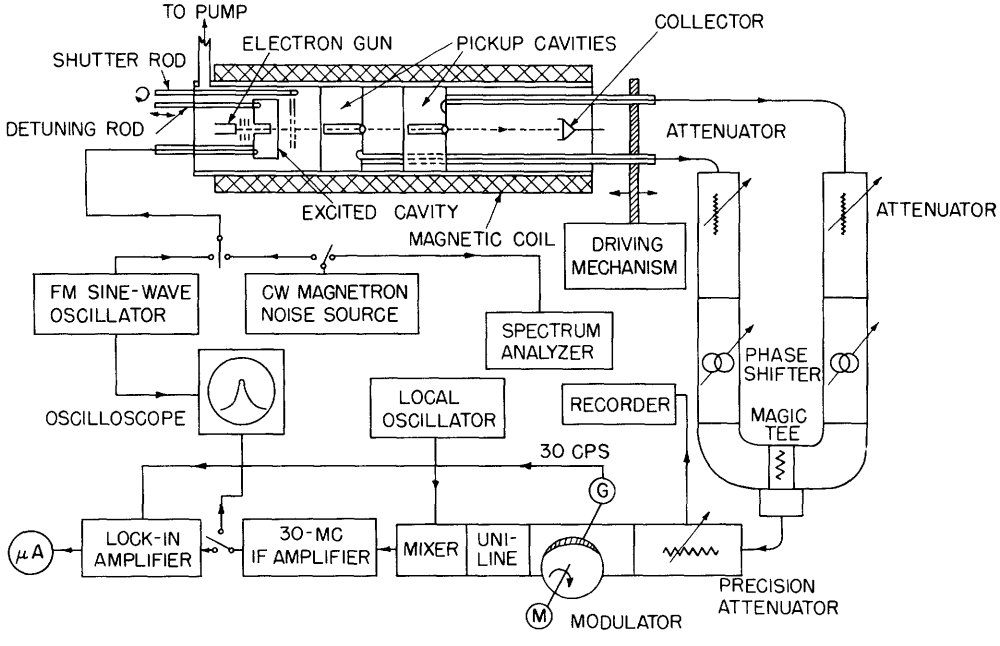

Fig. 7. Diagram of measuring system.

Table I. Characteristics of Pickup Cavities.

$\frac{R_s}{Q_o}$	130*
Q_o	2200
Q_L	500
M^2	0.49**
f_o	3080 mc ± 10 kc

*Measured by perturbation techniques with a steel ball of 0.016 inch diameter.

**For a 500-volt beam of 0.040 inch diameter. The cavity hole had a diameter of 0.080 inch and a gap length of 0.031 inch.

25 db below shot noise of the parallel-flow gun (V = 500 v, I_o = 350 μa), and of the RCA low-noise gun (V = 500 v, I_o = 260 μa) could be detected.

The noise measurement was performed by moving the cavities along the beam automatically. The cavity pickups were fed to the radiometer through a variable precision attenuator. While the cavities were moving along the electron beam the radiometer output was kept constant with the aid of continuous manual adjustments of the precision

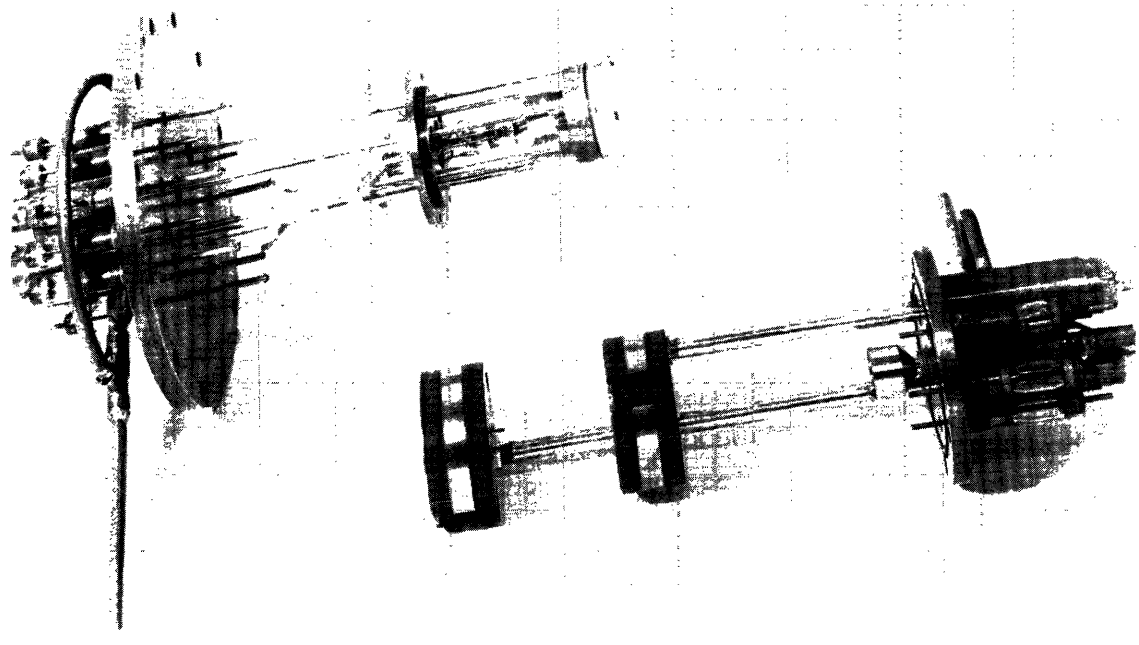

Fig. 8. Photograph of the electron-gun holder with RCA low-noise gun, excited cavity, and two pickup cavities.

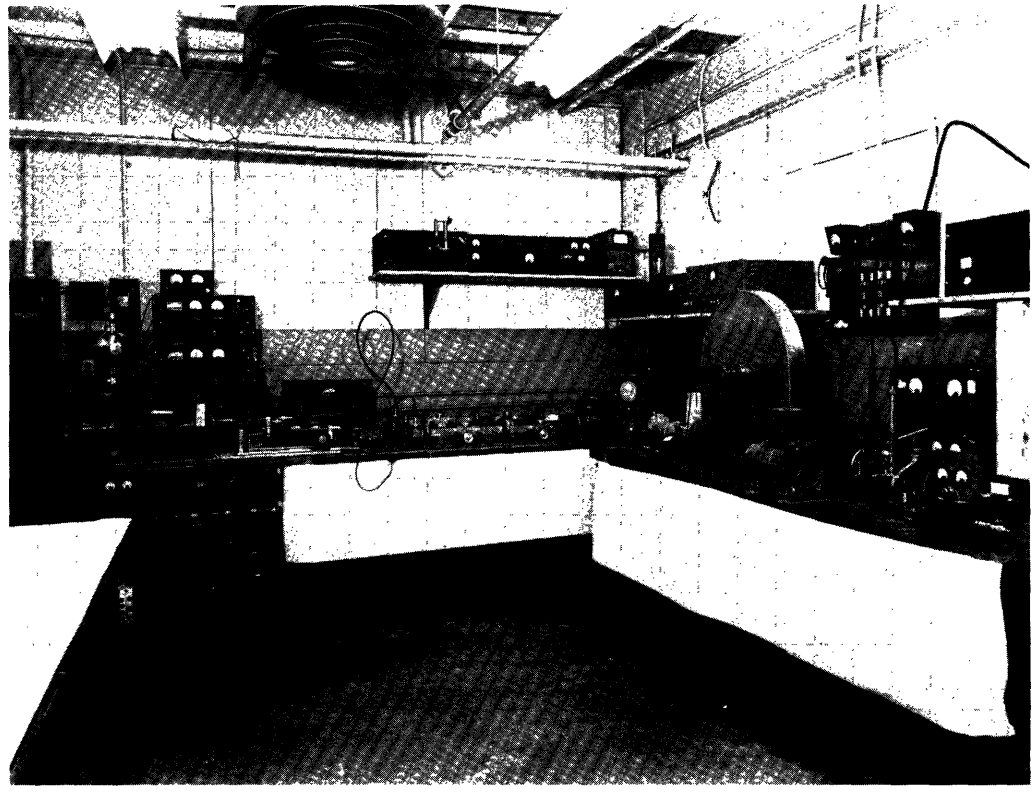

Fig. 9. Photograph of whole measuring system.

attenuator. The attenuator adjustments were simultaneously transmitted to an Esterline-Angus ammeter-recorder that plotted the variation of the electron-beam noise along the length of the beam.

The selective beam coupler was calibrated with the aid of a signal-excited cavity. This cavity was excited by either an FM signal generator or a cw magnetron noise source; thus the beam was modulated in a known way. The signal-excited cavity was fixed near the electron gun and was provided with a tuning-rod mechanism so that it could be detuned during the noise measurements. This cavity was made as small as possible so as to achieve a very low Q, approximately 60 at 3080 mc. The FM signal was fed to the excited cavity and the outputs of the two pickup cavities could be observed through the waveguide circuit and receiver on an oscilloscope. The cw magnetron, operating with a low plate voltage, generated a reasonably high-level noise. In our case the half-power bandwidth of this noise was 8.5 mc, as measured with the spectrum analyzer shown in Fig. 8.

In Fig. 8, from left to right, pictures of the large end plate, gun parts, excited cavity, two pickup cavities, and the small end plate are shown. Figure 9 shows a picture of the whole measuring system: from right to left, vacuum chamber with magnetic coil, cavity-driving mechanism, waveguide circuit, variable precision attenuator, modulator, and microwave receiver.

V. MEASURING PROCEDURE

The measuring procedure performed with this system can be divided into two parts; calibration of the selective beam coupler, and noise measurement.

5.1 METHOD OF CALIBRATION

Two methods of calibration can be used. One method employs a signal generator with a single frequency output. The other method employs an external white noise.

a. Sine-Wave Calibration

1. A sine-wave signal is fed into the excited cavity O. Its frequency is adjusted so that it is the same as the resonant frequency of cavities 1 and 2, and its input-signal level is reasonably higher than the noise level. Note that excitation of an electron beam by a short cavity gap leads to a perfect standing wave of current in the beam, and thus gives $|a_1| = |a_2|$.

2. Cavity 1 is moved along the beam. The standing-wave ratio ρ^2 and the plasma wavelength are measured.

3. Cavity 1 is fixed at the position of a current minimum where it does not have any effect on the beam. Then, cavity 2 alone is moved along the beam and the standing-wave ratio is measured.

4. The distance between cavities 1 and 2 is made equal to $\lambda_q/2$, and the attenuator and the phase shifter in the output line of cavity 1 are adjusted, until the output of the E-branch of the Magic Tee becomes zero. Then we can obtain the condition $\psi_c = \pi + \beta_e \Delta z$ and $L_c = 1$. L_c and ψ_c are standards of adjustment for the following measurements.

5. The distance between the two cavities is made equal to $\lambda_q/4$, and the phase shift is made equal to $\psi_a = \psi_c/2$ for case a, or $\psi_b = \psi_c/2 + \pi/2$ for case b. Then the attenuators in the output line of cavities 1 and 2 are adjusted to make the directivity of the selective beam coupler maximum. This is verified by observing the fluctuations of the output from the H-branch of the Magic Tee when the two cavities are moving together along the beam. The readings of the attenuator value, L_a and L_b, determine the value of r, since I_{ta} and I_{tb} with $x \ll 1$, are given as

$$I_{ta} = \sqrt{2Y_o}\,(ML_{2a})\left(\frac{G_L}{G_t}\right)\frac{2}{1+jx}\left\{\left(\frac{-jx}{2}\,r\right)a_1 e^{j\beta_q z_1} + a_2 e^{-j\beta_q z_1}\right\} e^{-j\beta_e z_1}$$

$$\text{for} \quad L_{1a} = (1-r)\,L_{2a} \tag{34}$$

$$I_{tb} = \sqrt{2Y_o}\,(ML_{2b})\left(\frac{G_L}{G_t}\right)\frac{2}{1+jx}\left\{a_1 e^{j\beta_q z_1} + \left(\frac{jx}{2}\,r\right) e^{-j\beta_q z_1}\right\} e^{-j\beta_e z_1}$$

$$\text{for} \quad L_{1b} = (1+r)\,L_{2b}$$

Note that the value of r does not have to be known, only the positions of the attenuator corresponding to L_a and L_b are required, unless the factor K_1/K_2 in Eq. 32 is calculated by using the value of r (see section 5.1c).

6. Under the conditions just described, the frequency characteristic of this equipment is obtained by varying the signal frequency. The signal level must be kept constant and the excited cavity must be tuned at each frequency, unless its Q is much lower than that of the pickup cavities, so that the excitation of the beam will be kept constant over the measured frequency range. Then, by integrating graphically the outputs $|I_{ta}|^2$ and $|I_{tb}|^2_{mean}$, obtained for each frequency with respect to ω, the value of K_1/K_2 in Eq. 32 can be obtained from

$$\frac{\sum |I_{ta}|^2_{mean}}{\sum |I_{tb}|^2_{mean}} = \frac{K_1\left(1 + a_a^2\right)}{K_2\left(1 + a_b^2\right)} \approx \frac{K_1}{K_2} \tag{35}$$

The error caused by omitting a_a^2 and a_b^2 is usually negligibly small compared with other errors.

b. White-Noise Calibration

This calibration method employs a white-noise source amplified to a level sufficiently larger than the beam noise and thermal noise. Since the white noise has a continuous-frequency spectrum, this method is more direct compared with the point-by-point method in the sine-wave calibration. In this case the Q of the excited cavity O should be much lower (say, one-tenth) than the Q's of the other measuring equipment, including the pickup cavities. When the external noise is not perfect white noise, but has some frequency characteristics (which was the case in our measurement), some error must be expected (see Section V). The calibration procedure is similar to that in the sine-wave calibration.

c. Calculation from the Values of the Circuit Parameters

The third method of determining the factor K_1/K_2 is to calculate it from Eq. 31, if the values of r, Q_L, ω_o, and the frequency response of the detector circuit are known (all of these values are measurable by standard methods).

5.2 BEAM-NOISE MEASUREMENT

For the noise measurement, the excited cavity must be detuned out of the resonant-frequency range of the equipment so that it will not affect the beam noise at the frequency of the measurement.

a. Measurements of S

$\Delta z = \lambda_q/2$, L_c and ψ_c are obtained from the calibration, and the standing-wave pattern is measured by moving the two cavities together along the beam. The absolute value of S is determined by a shot-noise calibration (5, 6, 7).

b. Measurement of Π

1. $\Delta z = \lambda_q/4$, L_a and ψ_a are set as they are obtained from the calibration, and the standing-wave pattern is measured. $\Sigma|I_{ta}|^2_{mean}$ is then obtained.

2. $z = \lambda_q/4$, L_b and ψ_b are set, and the value of $\Sigma|I_{tb}|^2_{mean}$ is obtained from the measurement of the standing-wave pattern.

3. The value of A_2/A_1 is calculated from

$$\frac{A_2}{A_1} = \left(\frac{K_2}{K_1}\right)\left(\frac{\sum |I_{ta}|^2_{mean}}{\sum |I_{tb}|^2_{mean}}\right) \tag{36}$$

Since we know the standing-wave ratio ρ^2 from the measurements of S, the value of Π/S can be obtained by using Eq. 23:

$$\frac{\Pi}{S} = \frac{1}{\frac{2\rho}{1+\rho^2}} \frac{1 - \frac{A_2}{A_1}}{1 + \frac{A_2}{A_1}} \tag{37}$$

VI. RESULTS OF MEASUREMENTS

Measurements of S and Π were performed on two different electron guns; one type was a parallel-flow gun which had one cathode-electrode and one anode; the other type was an RCA low-noise gun which had one beam-focusing electrode and three anodes. The cathode diameter of both types of guns was 0.040 inch. All experiments were performed at approximately 3080 mc. The magnetic field applied to the electron beam was approximately 420 gauss, and all partition current was below 0.05 per cent, except for some special cases. The pressure in the drift tube was 2 to 4 × 10^{-7} mm Hg.

6.1 MEASURED RESULTS ON THE RCA LOW-NOISE GUNS

The electrode arrangement and the potential distribution of the RCA low-noise gun are shown in Fig. 10. It consists of a beam-focusing section followed by two anodes of plane-parallel anodes at voltages E_3 and E_4. The beam-focusing section consists of a cathode, a beam-focusing electrode E_1, and a first anode E_2. This section may be considered as determining the noise parameters S and Π. Since the noise-smoothing section (E_3 and E_4) can be considered as a lossless transforming device, ideally, the applied voltage on its anodes should not affect the noise parameters (7).

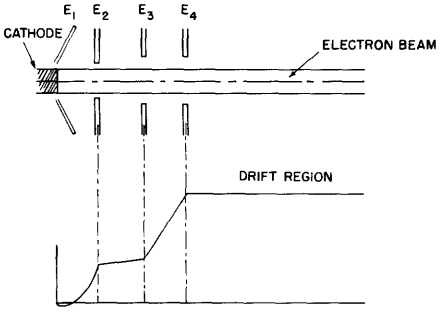

Fig. 10. Electrode arrangement and potential distribution of RCA low-noise gun.

The measurement was performed on two RCA low-noise guns of the same type (guns No. 1 and 2).

a. Measured Results on RCA Gun No. 1.

1. Calibration of the selective beam coupler

As mentioned in Section V, the beam was excited with sine-wave signals at the resonant frequency of the cavities, 3080 mc, and the signal standing-wave pattern along the beam that was picked up by cavity 1 was measured. Figure 11a shows the observed standing wave. The standing-wave ratio was higher than 35 db. From the distance between two successive deep minima, the plasma wavelength was determined as 24.3 ± 0.05 cm. The calculated value of the plasma wavelength (V_p = 500 v, I_c = 250 μa, and corrected for the finite beam diameter of 0.040 inch) was 24.6 cm. Figure 11b and c shows the outputs, $|I_{ta}|^2$ and $|I_{tb}|^2$, of the selective beam coupler at the resonant frequency. The residual standing-wave ratios were 1.6 db for case a (Fig. 11b), and 2.0 db for case b (Fig. 11c). From the measured value of the attenuation, we obtained the value of the equivalent series resistance of cavity 1 as $r \approx 0.45$. This value was

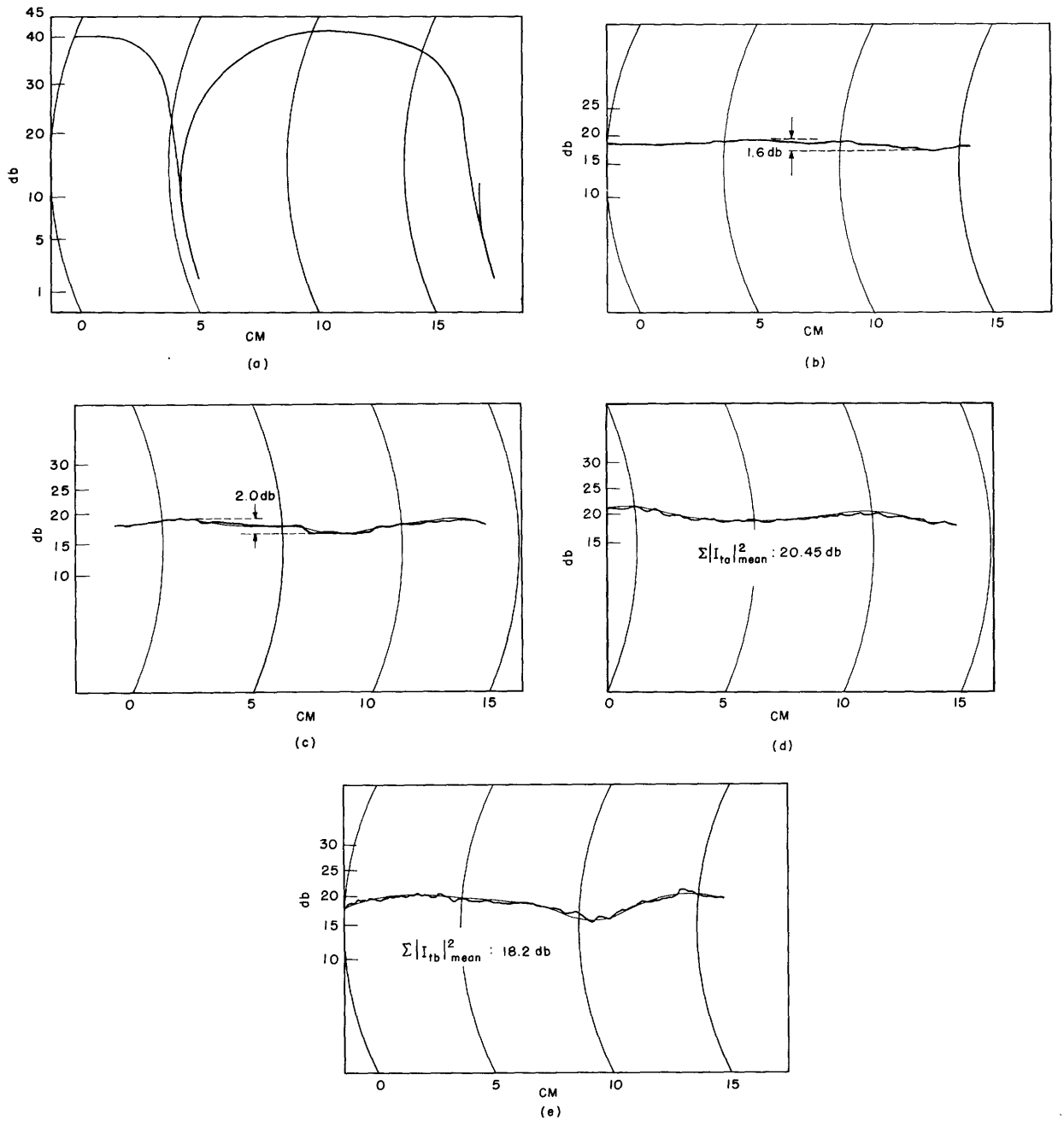

Fig. 11. Measured curves obtained in the calibration of the system on RCA low-noise gun No. 1.

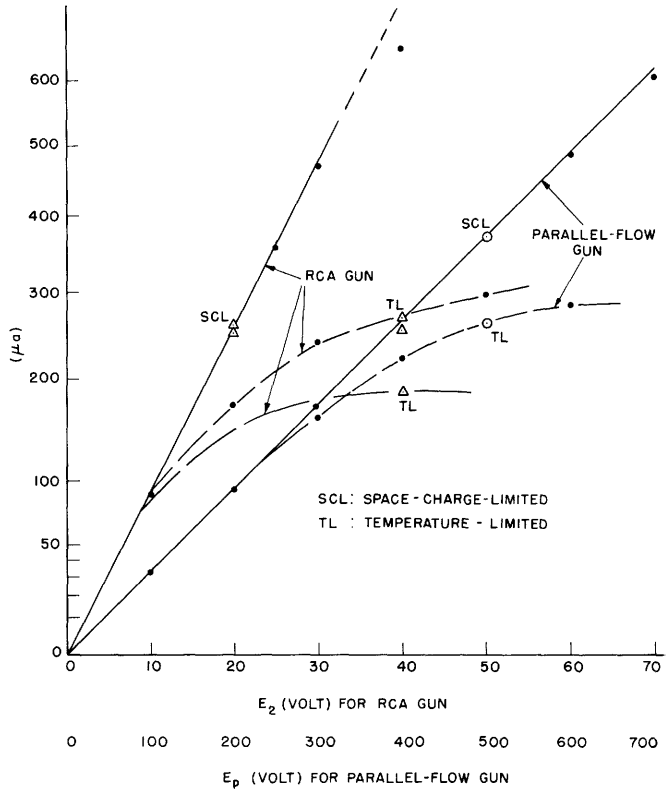

Fig. 12. $I_p - V_p$ characteristics (two-third power curves).

theoretically calculated as 0.465 from the independently measured value of R_s and from the computed values of Y_o and M^2.

Next, the coefficient K_2/K_1 was determined with the external noise. Figure 11d and e shows $\Sigma|I_{ta}|^2$ and $\Sigma|I_{tb}|^2$. From the mean values of these two standing waves, K_2/K_1 was determined as 0.595. The theoretical value of K_2/K_1 computed from Eq. A-7 was 0.598.

2. Beam-noise measurements

The beam-noise measurements were performed under two different conditions, one in the space-charge-limited region, and the other in the temperature-limited region.

a. Measurement in the space-charge-limited region. This measurement was carried out two hours after activation. The cathode current was kept at 250 ± 5 μa at the fixed voltages: E_1 = 0 v, E_2 = 20 v, and E_4 = 500 v (see Fig. 10). Data were taken with variable voltage applied on the second anode, E_3 = 50, 70, and 90 v. This condition was pointed on the two-third power curve (Fig. 12) and was verified as the space-charge-limited region.

Figure 13a-1, a-2, and a-3 shows the noise standing-wave patterns as picked up by cavity 1. The average level of the noise-current standing wave in db below shot noise, A, was determined by shot-noise calibration with a shutter rod (7). The value

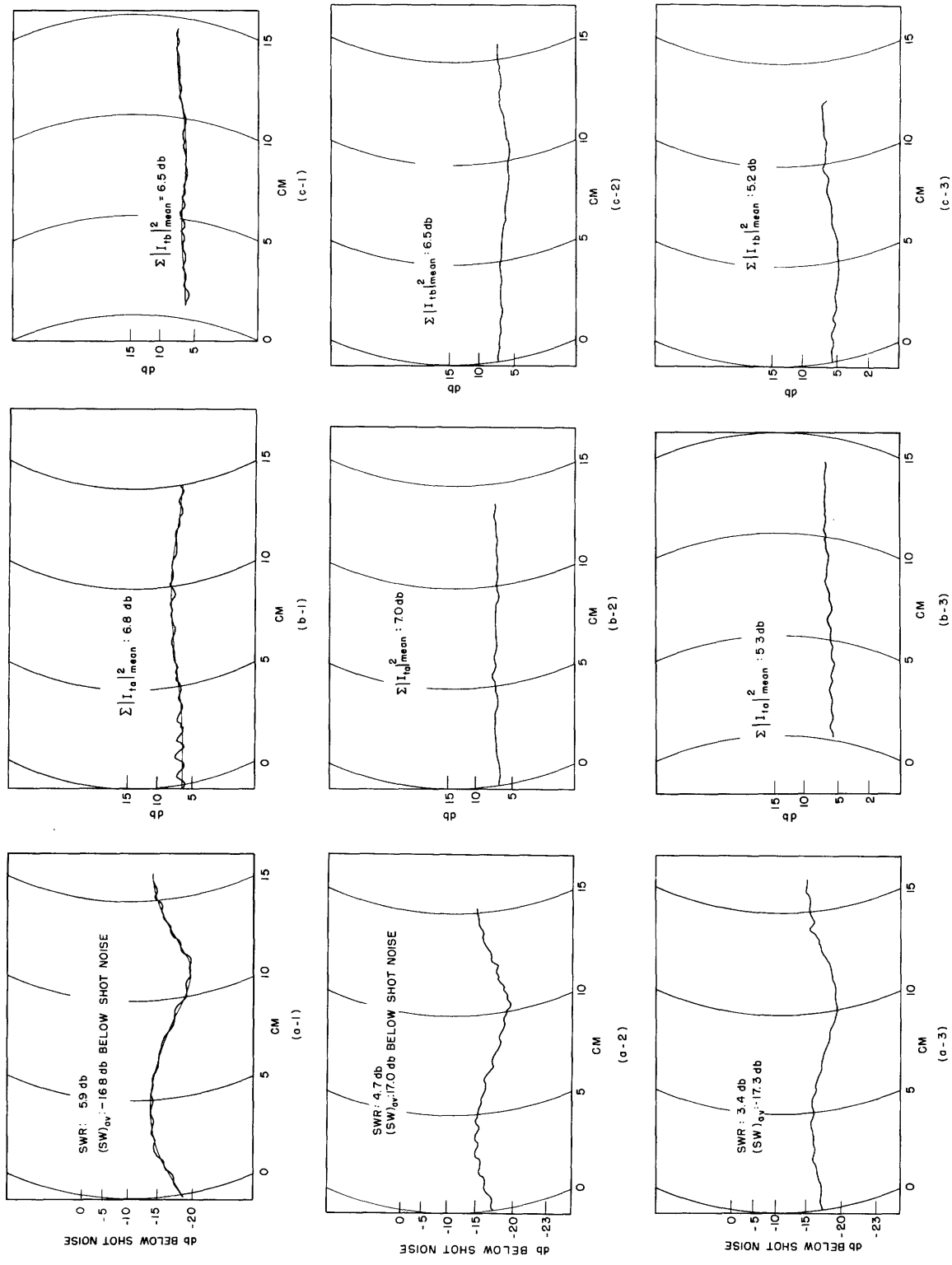

Fig. 13. Measured curves on RCA gun No. 1 in space-charge-limited region.

of S can be computed by using

$$S = -\frac{V_o}{a}\frac{\lambda_e}{\lambda_q} \tag{38}$$

where e is the electron charge, and $a = 10 \log_{10} A$.

Figure 13b-1, b-2, and b-3 shows the outputs of the beam selective coupler for case a, $\Sigma|I_{ta}|^2$, and Fig. 13c-1, c-2, and c-3 shows the outputs for case b, $\Sigma|I_{tb}|^2$. From the arithmetic mean value of these curves, A_2/A_1 was obtained, since the coefficient K_2/K_1 had been calibrated.

However, it sometimes happened that the standing wave slightly increased linearly with the distance between the cathode and the pickup cavities. To eliminate the uncertainty in the determination of the mean value, the mean value at a fixed reference point as near as possible to the cathode (1.75 inches from the last anode) was taken. This was done, as shown in Appendix IV, by measuring the slope of the standing-wave pattern, and by assuming an additional distributed noise source along the beam.

The apparent values of A_2/A_1 that were obtained by this procedure included the additional terms from the finite selectivity of the selective beam coupler caused by the equivalent series resistance, r, of cavity 1, and the external thermal noise. The true value of A_2/A_1 was computed by using Eq. A-8. The difference between the apparent value and the true value was within 10 per cent.

From the measured standing-wave ratio, ρ, of the beam noise (Fig. 13a-1, a-2, and a-3) and the modified values of A_2/A_1, Π/S was computed by using Eq. 37. Table II shows the average standing-wave-ratio level of the standing wave below shot noise, S, the apparent and true values of A_2/A_1, and Π/S. Since the noise parameters S and Π must be constant for the variation of the applied voltage on the second anode at the fixed voltage on the other anode, the mean values of S and Π are shown in Table II. Also, the probable error in the S- and Π-measurements was computed, as shown in Section VII. The probable values of S and Π/S were determined as

$$S = 8.81 \times 10^{-21} \pm 8 \text{ per cent} \quad \text{(watt-sec)}$$

$$\frac{\Pi}{S} = 0.21 \pm 0.04$$

b. Measurement in the temperature-limited region. The noise measurements in the temperature-limited region were performed by lowering the heater voltage and using the applied voltage on the first anode (40 v) approximately 40 hours after activation (see Fig. 12). The cathode current was almost the same, 250 μa, as in the measurements in the space-charge-limited region. The standing wave and the outputs of the selective coupler are shown in Fig. 14. Table III gives the measured results. The probable values of S and Π/S are:

Table II. Measured Data on RCA Gun No. 1 in Space-Charge-Limited Region.

E_3	SWR (db)	$(SW)_{av}$ (db below shot noise)	S (watt-sec)	$\left(\frac{A_2}{A_1}\right)_{ap}$	$\left(\frac{A_2}{A_1}\right)_{true}$	$\frac{\Pi}{S}$
50 v	5.9	-16.8	9.32×10^{-21}	0.638	0.682	0.232
70 v	4.7	-17.0	8.86×10^{-21}	0.660	0.717	0.190
90 v	3.4	-17.3	8.23×10^{-21}	0.612	0.672	0.212
Mean Value and Maximum Deviation			8.81×10^{-21} + 5.9% - 6.6%			0.211 ± 10%
Probable Error			8%			19.5%

Table III. Measured Data on RCA Gun No. 1 in Temperature-Limited Region.

	SWR (db)	$(SW)_{av}$ (db below shot noise)	S (watt-sec)	$\left(\frac{A_2}{A_1}\right)_{ap}$	$\left(\frac{A_2}{A_1}\right)_{true}$	$\frac{\Pi}{S}$	Probable Error in Measurement of $\frac{\Pi}{S}$
E_1 = 0 E_2 = 40 v E_3 = 70 v E_4 = 500 v	3.7	-15.6	1.22×10^{-20}	0.968	1.048	-0.024	152%
E_1 = 4 v E_2 = 25 v E_3 = 70 v E_4 = 500 v	4.8	-15.9	1.15×10^{-20}	1.14	1.19	-0.10	42.5%

Table IV. λ_q, r, and $\frac{K_2}{K_1}$ for RCA Gun No. 2.

	Measured Value	Theoretical Value
λ_q	24.0 cm	23.7 cm
r	0.50	0.480
$\frac{K_2}{K_1}$	0.550	0.567

Table V. Measured Data on RCA Gun No. 2 in Space-Charge-Limited Region.

E_3	SWR (db)	$(SW)_{av}$ (db below shot noise)	S (watt-sec)	$\left(\frac{A_2}{A_1}\right)_{ap}$	$\left(\frac{A_2}{A_1}\right)_{true}$	$\frac{\Pi}{S}$
50 v	4.4	-16.5	1.01×10^{-20}	0.550	0.577	0.303
70 v	2.8	-16.9	9.24×10^{-21}	0.539	0.572	0.286
90 v	2.2	-17.0	9.02×10^{-21}	0.578	0.620	0.240
Mean Value and Maximum Deviation			9.42×10^{-21} + 7.4% - 4.2%			0.276 +11% -13%
Probable Error			8%			13.2%

$$S = 1.22 \times 10^{-20} \pm 8 \text{ per cent} \quad \text{(watt-sec)}$$

$$\frac{\Pi}{S} = -0.02 \pm 0.04$$

Note that Π/S was almost zero, as the simple theory predicted, and S increased approximately 1.5 db, as compared with the value in the space-charge-limited region.

Next, we shall show a measure that was taken after the cathode started to die out, 80 hours after activation. Slightly positive voltage (+4 v) was applied to the beam-focusing electrode E_1 (the partition current 5 μa flowed into this electrode), and the cathode current was the same, 250 μa. Figure 15 shows the noise standing wave and the outputs of the selective beam coupler. The measured results are given in Table III. The following values were obtained:

$$S = 1.15 \times 10^{-20} \pm 8 \text{ per cent} \quad \text{(watt-sec)}$$

$$\frac{\Pi}{S} = -0.10 \pm 0.04$$

It is interesting to note that Π/S went down to negative.

b. Measured Results on RCA Gun No. 2

1. Calibration of the selective beam coupler

The same calibration procedure was performed as before. The measured values of the plasma wavelength of the cathode current, 270 μa, the equivalent series resistance of cavity 1, r, the coefficient K_2/K_1, and their theoretical values are given in Table IV. Figure 16 shows the outputs of the selective beam coupler with the external noise excitation.

2. Beam-noise measurements

The noise measurements were performed in the space-charge-limited region and in the temperature-limited region.

a. Measurement in the space-charge-limited region. The measurement was made 50 hours after activation. The cathode current was kept to 260 ± 5 μa at $E_1 = 0$, $E_2 = 20$ v, and $E_4 = 500$ v, variable voltages of 50 v, 70 v, and 90 v being applied on E_3.

Figure 17 shows the noise standing wave and the outputs of the selective beam coupler, $\Sigma|I_{ta}|^2$ and $\Sigma|I_{tb}|^2$. The mean values of the outputs of the selective coupler, $\Sigma|I_{ta}|^2_{mean}$ and $\Sigma|I_{tb}|^2_{mean}$, were taken at the same reference point (1.75 inches from the last anode). All summarized data are given in Table V. From the mean value of these data, the probable noise parameters were determined as

$$S = 9.42 \times 10^{-21} \pm 8 \text{ per cent} \quad \text{(watt-sec)}$$

$$\frac{\Pi}{S} = 0.28 \ (\pm 0.036)$$

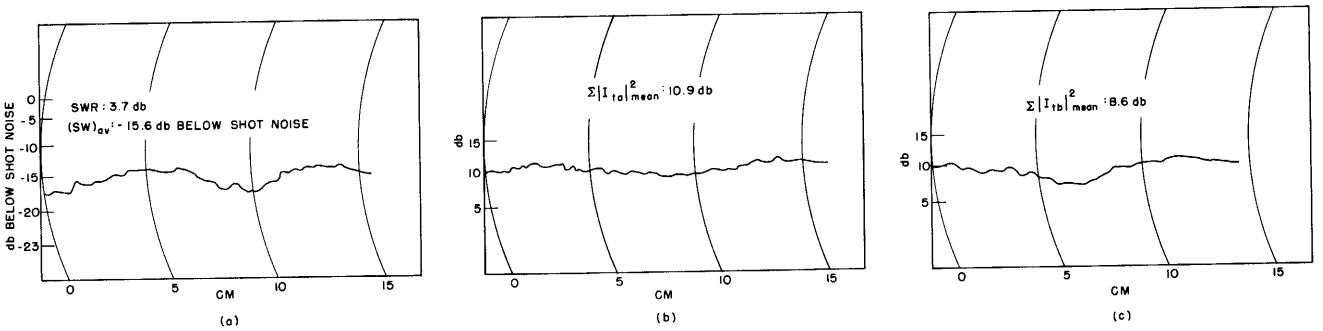

Fig. 14. Measured curves on RCA gun No. 1 in temperature-limited region.

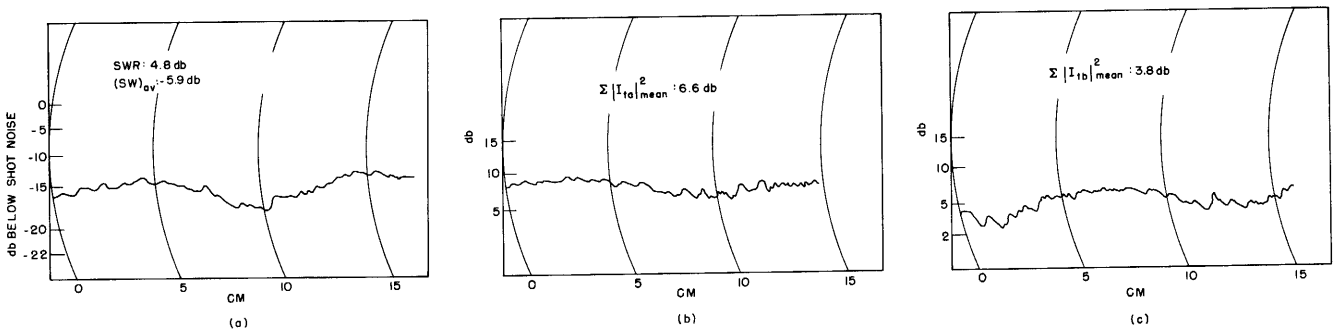

Fig. 15. Measured curves on RCA gun No. 1 in temperature-limited region, after the cathode began to die out.

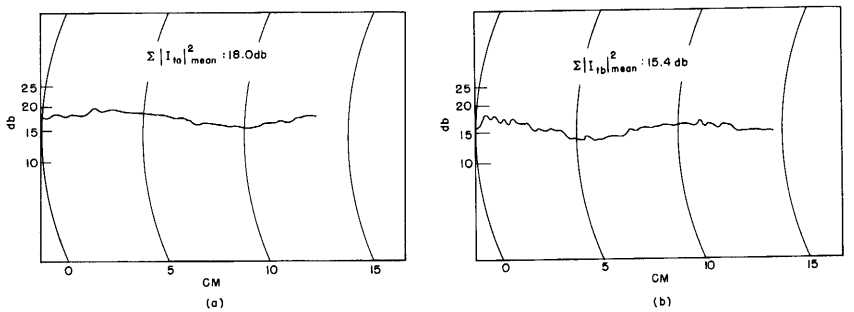

Fig. 16. Measured curves obtained in the calibration of the system on RCA gun No. 2.

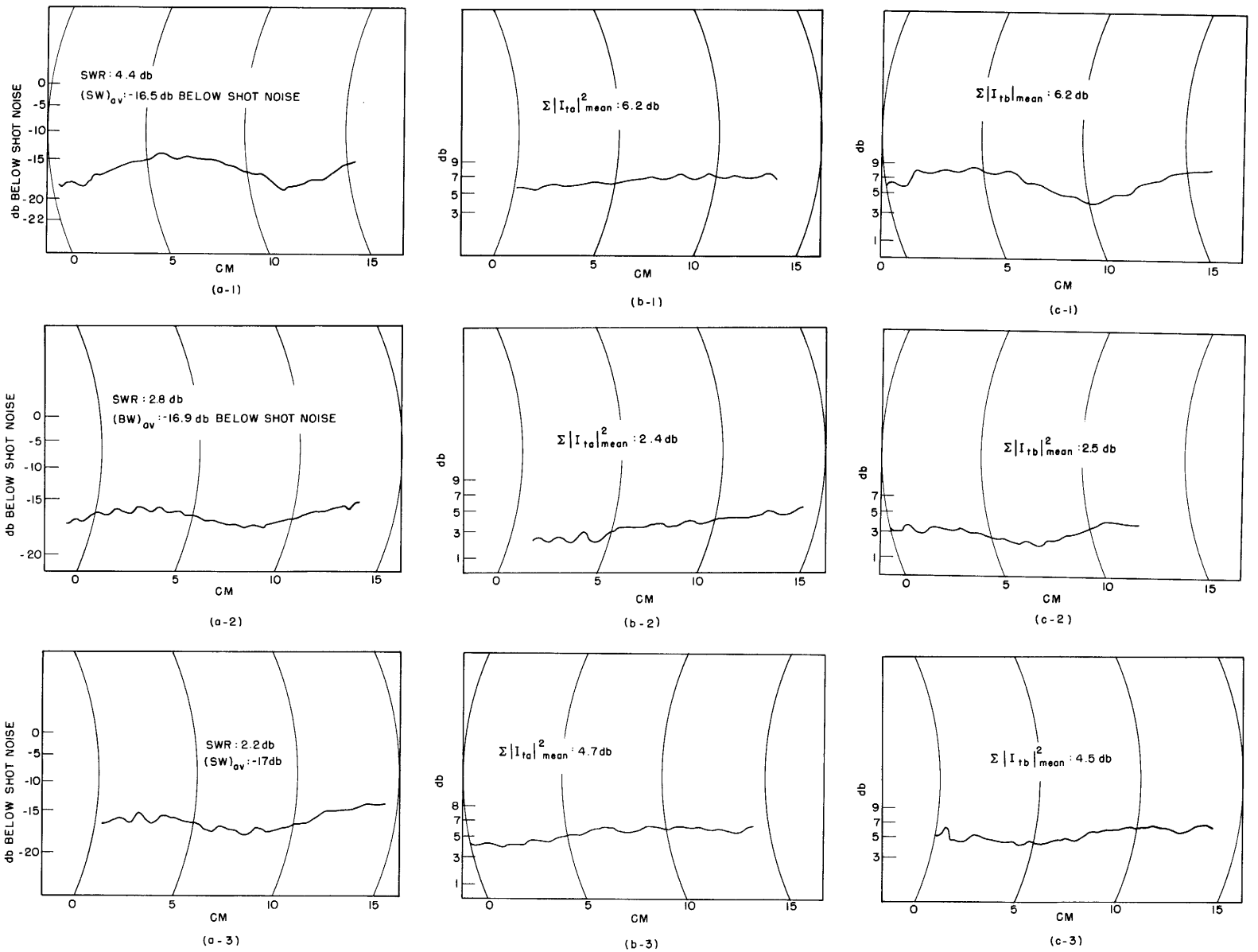

Fig. 17. Measured curves on RCA gun No. 2 in space-charge-limited region.

Another measurement was performed by changing the applied voltage on the beam-focusing electrode E_1; the cathode current was kept constant by adjusting the applied voltage on the first anode. The measured curves are shown in Fig. 18. The summarized results are given in Table VI. In this case we would expect the noise parameters to change, because the field distribution near the potential minimum changes in accordance with the variation of the focusing electrode and first-anode voltage. The measured results show that the value of Π/S increased slightly with the decrease of the applied voltage of the beam-focusing electrode E_1. In the case of $E_1 = +10$ v, Π/S went down to negative and S increased approximately 2 db. Since the partition current flowing to E_1 was 6 μa (total cathode current, 265 μa), it is unknown whether the change of field distribution or the partition current had the main effect on the change of noise parameters.

b. Measurements in temperature-limited region. One series of measurements in the temperature-limited region was performed immediately (within 2 hours) after activation. The cathode current was kept at 265 ± 10 μa at $E_1 = 0$, $E_2 = 40$ v, $E_4 = 500$ v with applied variable voltages on E_3 of 50 v, 70 v, and 90 v. (See Fig. 12.) The noise standing wave and output of the selective beam coupler are shown in Fig. 19. The summarized measured data are given in Table VII. From these data the probable value of the noise parameters was

$$S = 1.16 \times 10^{-20} \pm 8 \text{ per cent} \quad \text{(watt-sec)}$$

$$\frac{\Pi}{S} = -0.13 \pm 0.04$$

Note that Π/S was definitely negative, and S was approximately 1 db higher than the value taken 50 hours after activation in the space-charge-limited region. Another measurement was performed 10 hours after activation. The cathode current was relatively small (180 μa) at $E_1 = 0$, $E_2 = 40$ v, $E_3 = 70$ v, and $E_4 = 500$ v; this condition was the temperature-limited region, as seen from Fig. 12. The measured curves and data are given in Fig. 20 and in Table VIII. Π/S was almost zero (0.03 ± 0.05).

6.2 MEASURED RESULTS ON THE PARALLEL-FLOW GUN

The parallel-flow gun had no noise-transforming section, but consisted only of a triode section, cathode, cathode-electrode E_1, and anode E_2.

a. Calibration of the Selective Coupler

The same calibration procedure was performed as in the measurements on the RCA guns. The standing wave and the outputs of the selective coupler with the sine-wave signal and external-noise excitation are illustrated in Fig. 21. The coefficient K_2/K_1 was determined as 0.708 at $E_1 = 0$, $E_2 = 500$ v, and $I_c = 370$ μa.

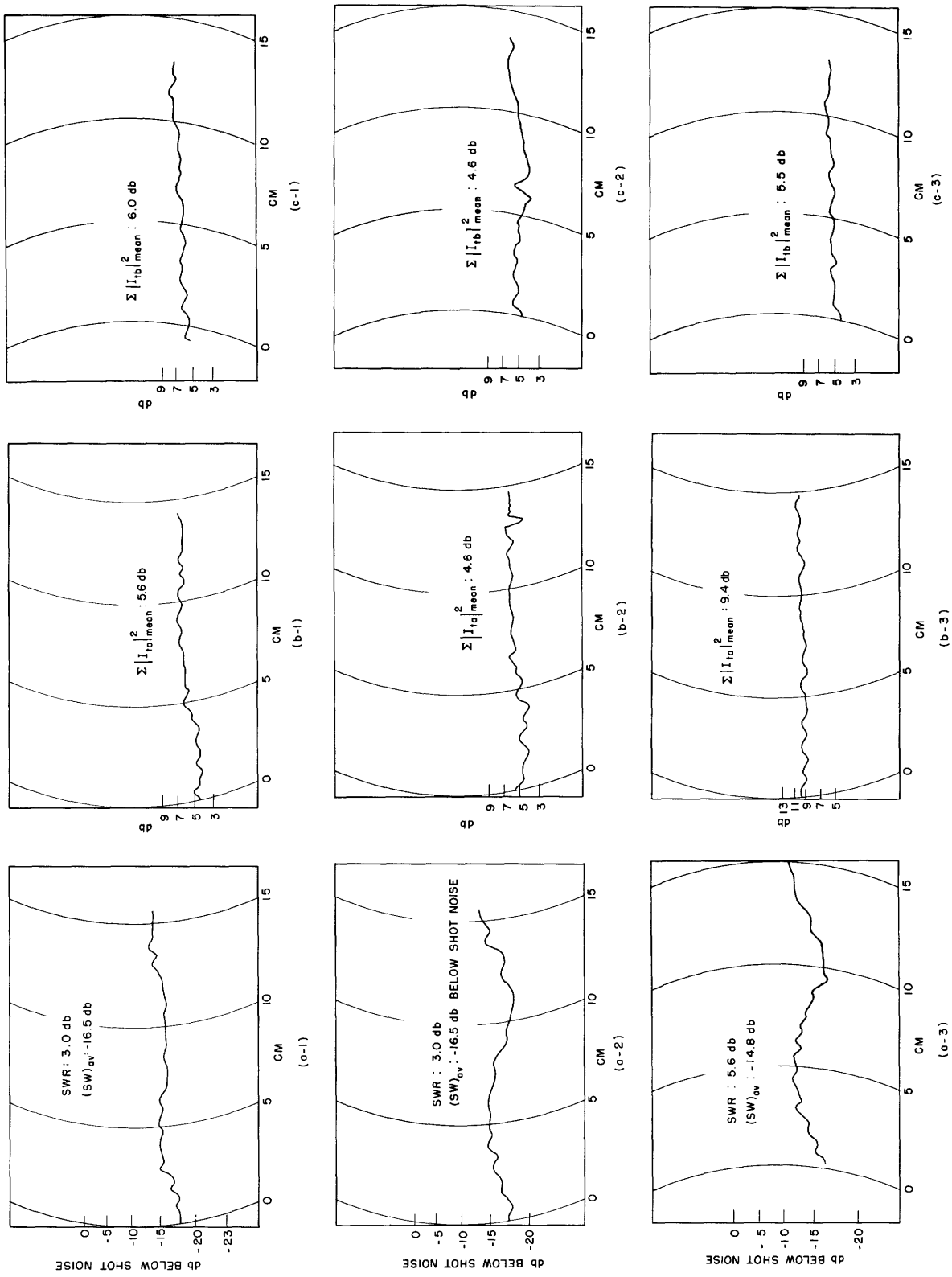

Fig. 18. Measured curves on RCA gun No. 2 with various voltages applied on the focusing electrode.

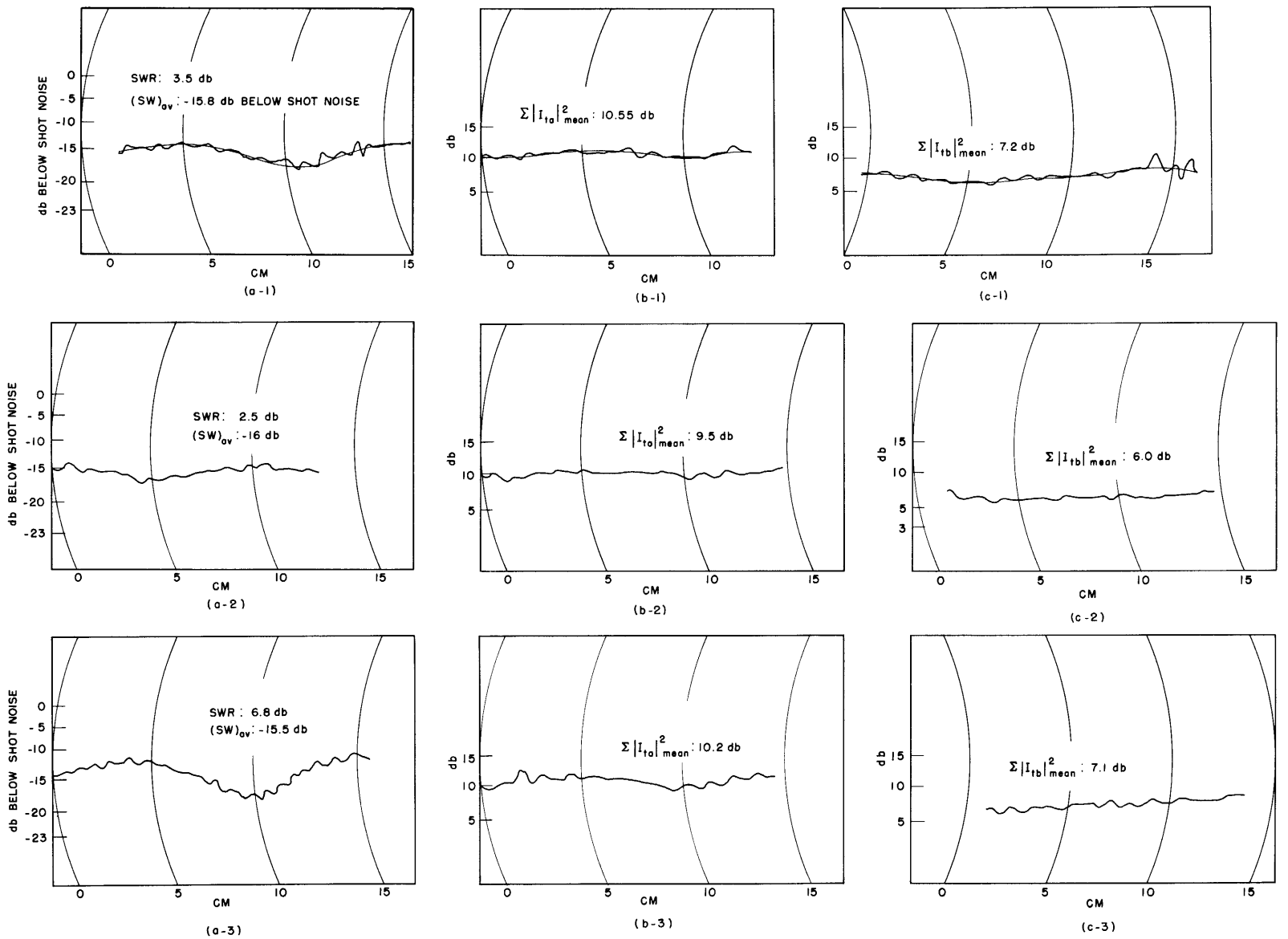

Fig. 19. Measured curves on RCA gun No. 2 in temperature-limited region, within 2 hours after activation.

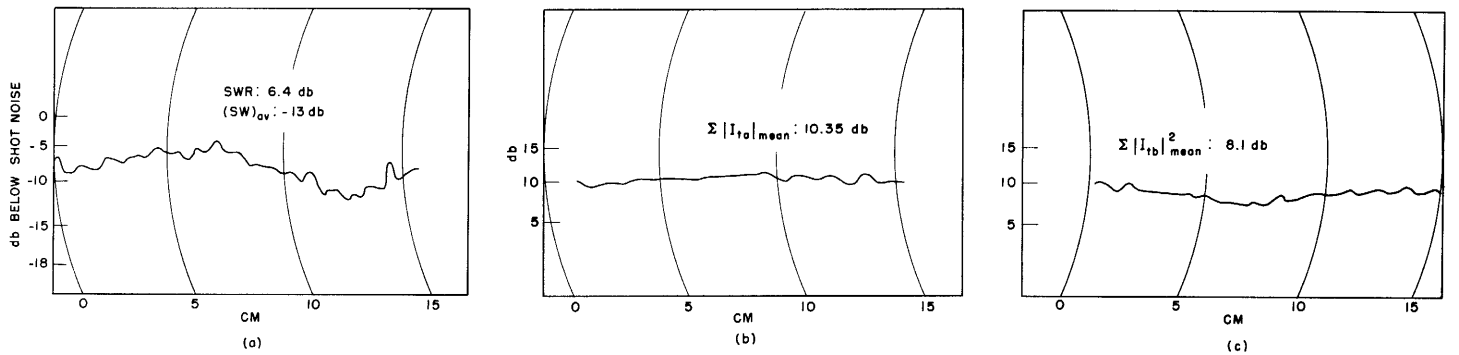

Fig. 20. Measured curves on RCA gun No. 2 in temperature-limited region, 10 hours after activation.

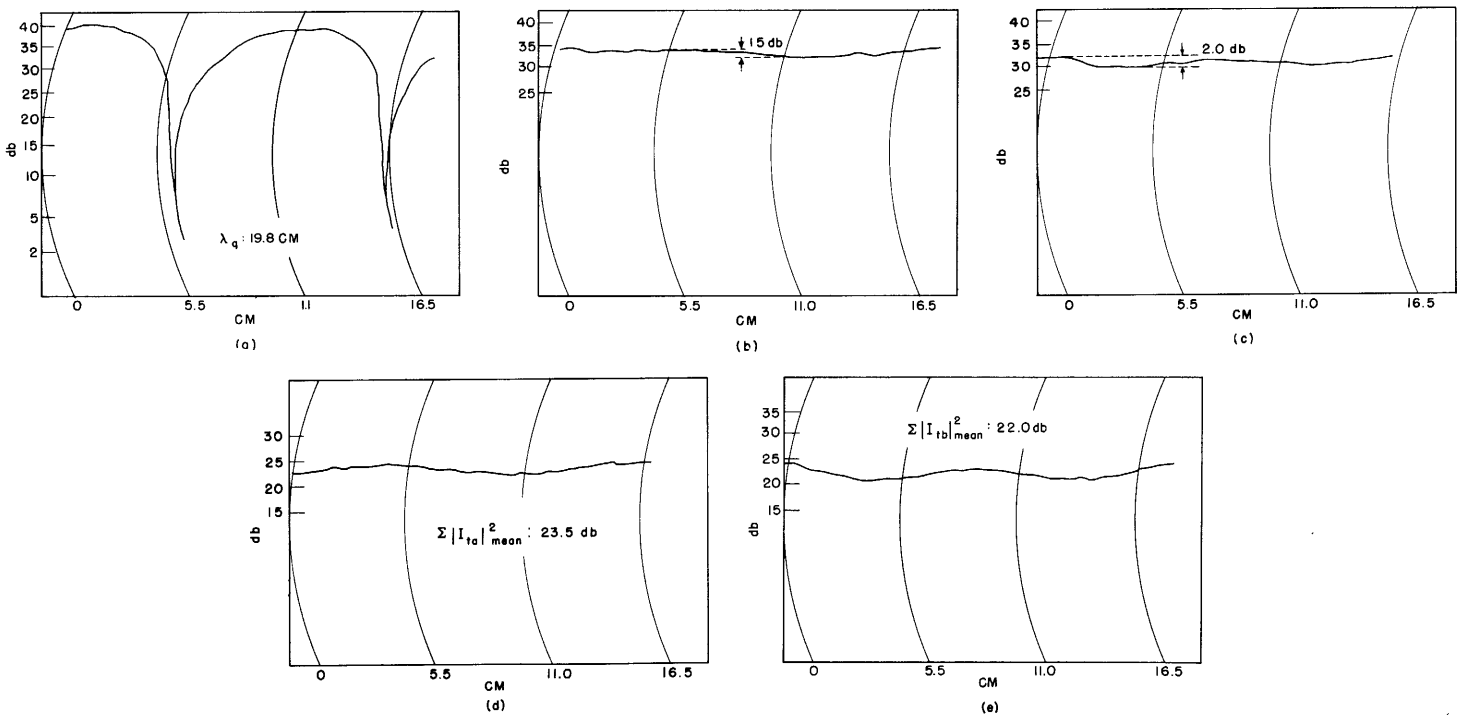

Fig. 21. Measured curves obtained in calibration of system with parallel-flow gun.

Table VI. Noise Parameters with a Change in Voltage Applied to the Beam-Focusing Electrode.

(All data were taken at I_p = 265 μa, E_3 = 70 v, and E_4 = 500 v.)

	E_1 = -3 v E_2 = 27 v	E_1 = 0 E_2 = 20	E_1 = 5 v E_2 = 18 v	E_1 = 10 v * E_2 = 15 v
SWR (db)	3.0	2.2	3.0	5.6
$(SW)_{av}$ (db below shot noise)	-16.5	-16.9	-16.5	-14.8
S (watt-sec)	1.01×10^{-20}	9.24×10^{-21}	1.01×10^{-20}	1.50×10^{-20}
Probable Error in Measurement of S	8%	8%	8%	8%
$\left(\frac{A_2}{A_1}\right)_{ap}$	0.501	0.539	0.550	1.35
$\left(\frac{A_2}{A_1}\right)_{true}$	0.542	0.572	0.584	1.45
$\frac{\Pi}{S}$	0.318	0.286	0.280	-0.221
Probable Error in Measurement of $\frac{\Pi}{S}$	12%	12.4%	12%	19%
Probable Value of $\frac{\Pi}{S}$	0.32 ± 0.04	0.29 ± 0.04	0.28 ± 0.03	-0.22 ± 0.04

*Partition current flowing into E_1 was 6 μa.

Table VII. Measured Data on RCA Gun No. 2 in Temperature-Limited Region, 2 Hours after Activation.

E_3	SWR (db)	$(SW)_{av}$ (db below shot noise)	S(watt-sec)	$\left(\frac{A_2}{A_1}\right)_{ap}$	$\left(\frac{A_2}{A_1}\right)_{true}$	$\frac{\Pi}{S}$
50 v	3.5	-15.8	1.17×10^{-20}	1.18	1.26	-0.124
70 v	2.5	-16.0	1.12×10^{-20}	1.23	1.34	-0.151
90 v	6.8	-15.5	1.25×10^{-20}	1.12	1.18	-0.108
Mean Value and Maximum Deviation			1.16×10^{-20} + 8% - 3.5%			-0.126 + 20% - 14%
Probable Error			8%			32%

Table VIII. Measured Data on RCA Gun No. 2 in Temperature-Limited Region, 10 hours after Activation.

SWR (db)	6.4
$(SW)_{av}$ (db below shot noise)	-13
S(watt-sec)	1.89×10^{-20}
$\left(\frac{A_2}{A_1}\right)_{ap}$	0.925
$\left(\frac{A_2}{A_1}\right)_{true}$	0.953
$\frac{\Pi}{S}$	0.03
Probable Error in Measurement of $\frac{\Pi}{S}$	153%

Table IX. Measured Data on Parallel-Flow Gun.

	Space-Charge-Limited Region I_p = 360 μa	Temperature-Limited Region I_p = 260 μa
SWR (db)	12.8	14.5
$(SW)_{av}$ (db below shot noise)	-14.8	-14.9
S (watt-sec)	175×10^{-20}	1.40×10^{-20}
$\left(\frac{A_2}{A_1}\right)_{ap}$	0.778	0.940
$\left(\frac{A_2}{A_1}\right)_{true}$	0.798	0.970
$\frac{\Pi}{S}$	0.258	0.04
Probable Error in Measurement of $\frac{\Pi}{S}$	24%	190%

Table X. $\frac{\Pi}{S}$ for Several Assumed Standing-Wave Ratios.

SWR (db)	Space-Charge-Limited Region	Temperature-Limited Region
13	0.26	
15	0.37	0.05
20	0.56	0.08

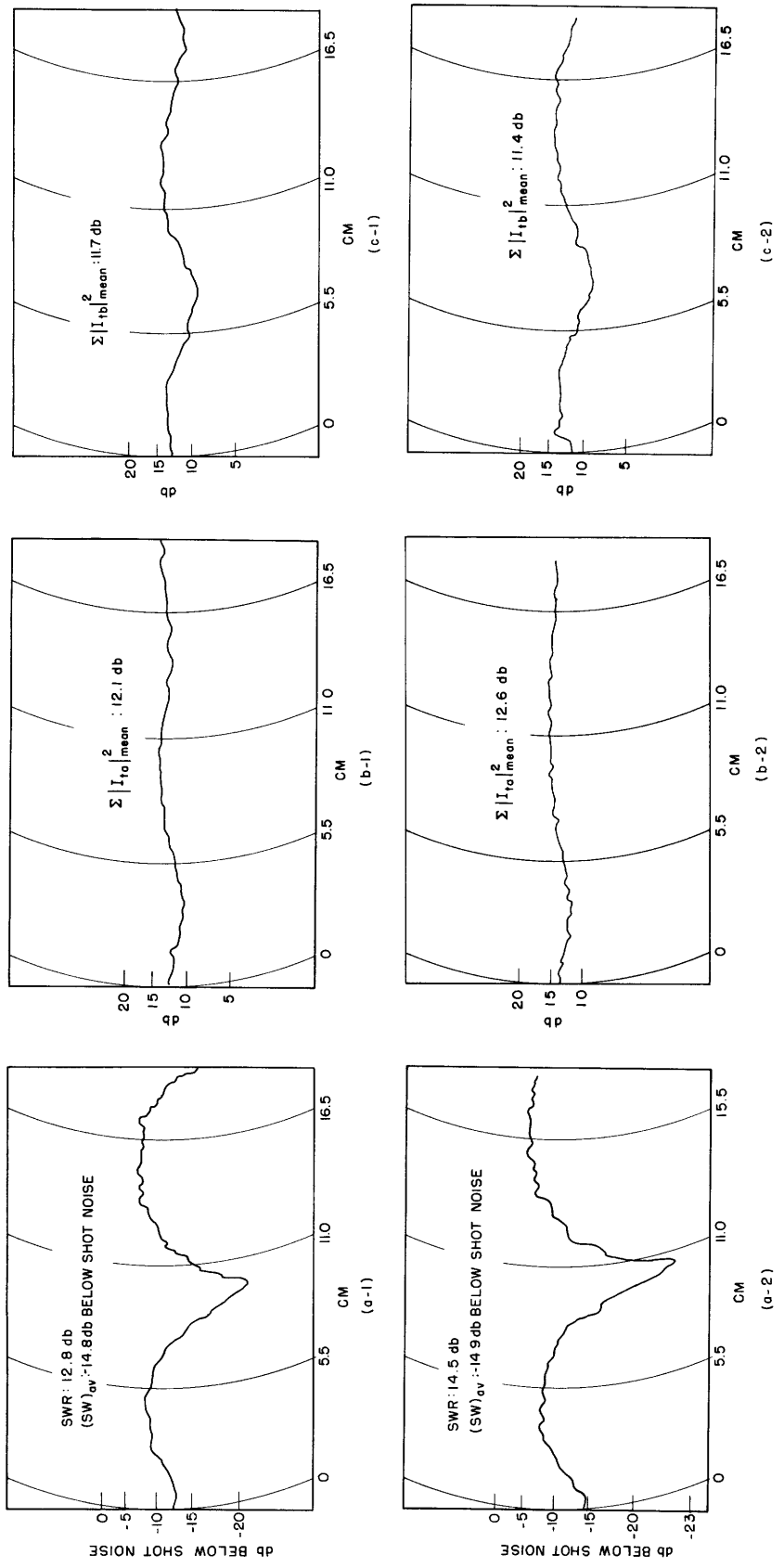

Fig. 22. Measured curves in parallel-flow gun.

b. Beam-Noise Measurements

Two measurements were performed: one in the space-charge-limited region, and the other in the temperature-limited region (see Fig. 12). The measured curves and summarized data are given in Fig. 22 and in Table IX. Mean values of the outputs of the selective coupler, $\Sigma|I_{ta}|^2_{mean}$ and $\Sigma|I_{tb}|^2_{mean}$, were taken at a fixed reference point (1.500 inches from the anode) by the same procedure as with the RCA guns. From Table X, probable values of Π/S were determined as

$$\frac{\Pi}{S} = 0.26 \pm 0.06 \quad \text{for space-charge-limited region}$$

$$\frac{\Pi}{S} = 0.04 \pm 0.08 \quad \text{for temperature-limited region}$$

Note, however, that the measured noise standing-wave ratio was very high compared with that of the RCA low-noise gun. In these cases small amounts of higher-order modes, or additional noise, might have a serious effect on the standing-wave ratio. It can be assumed that the true standing-wave ratio for the fundamental mode was much greater than the measured value. In other words, the real standing-wave ratio could not be determined in this measurement. Therefore the S and Π/S measured here might undergo a serious change, but the value of A_2/A_1 would not be seriously affected by the existence of the higher-order mode or by additional noise (see Section V). The values of Π/S for various assumed standing-wave ratios are given in Table X. S will decrease with an increase in the standing-wave ratio.

VII. ERRORS IN MEASUREMENTS

7.1 ERROR IN THE MEASUREMENT OF Π/S

We shall consider, first, the error in the measurement of Π/S, since this error is given by

$$\frac{\delta\left(\frac{\Pi}{S}\right)}{\left(\frac{\Pi}{S}\right)} = \frac{\rho^2 - 1}{\rho^2 + 1}\,\frac{\delta\rho}{\rho} + \frac{-2\left(\frac{A_2}{A_1}\right)}{1-\left(\frac{A_2}{A_1}\right)^2}\,\frac{\delta\left(\frac{A_2}{A_1}\right)}{\left(\frac{A_2}{A_1}\right)} \tag{39}$$

where δ denotes deviation. The causes of this error fall into two groups: the error caused by the error in the measurement of ρ, $\delta\rho$, and the error caused by the error in the measurement of A_2/A_1, $\delta\left(\frac{A_2}{A_1}\right)$.

a. Error from $\delta\rho$ (Standing-Wave Ratio)

The measurement of the standing-wave ratio, ρ, is carried out with essentially the same methods that have been previously described (5, 6, 7). Since the experimental error of ρ is usually within 0.4 db, the first term in Eq. 39 amounts to 5 per cent, even in the worst case (infinite standing-wave ratio).

b. Error from $\delta\left(\frac{A_2}{A_1}\right)$

The error in the measurement of A_2/A_1 is much more complicated and can be classified as follows:

1. Error from maladjustment in the selective beam coupler. When the selective beam coupler is not properly adjusted, and therefore has imperfect selectivity at the resonant frequency of the two pickup cavities, some error will be introduced into the measurement of A_2/A_1. These maladjustments may be caused by inserting an improper attenuation value (let the attenuation value be $L' = 1 \pm r + \Delta$, Δ being the deviation from the proper value), by taking an improper phase-shift value (let δ be the deviation from the proper value in radians), and by the deviation of the distance between the two cavities from $1/4\ \lambda_q$.

Let us take account of the first and second causes of errors. After some mathematical manipulations, their effect upon the selectivity can be expressed as follows: for case a, the coefficient of the unwanted term A is given by

$$\frac{r^2}{8(1+\alpha)} + \frac{\Delta^2 + (1-r)^2\delta^2}{4} + \frac{2r\Delta - r(2-3r)\delta^2}{8(1+\alpha)} \tag{40}$$

instead of by $\frac{r^2}{8(1+\alpha)}$ in Eq. A-5. For case b, the coefficient of the unwanted term A_2

is given by

$$\frac{r^2}{8(1+\alpha)} + \frac{\Delta^2 + (1+r)^2\delta^2}{4} - \frac{2r\Delta - r(2+3r)\delta^2}{8(1+\alpha)} \tag{41}$$

instead of by $\frac{r^2}{8(1+\alpha)}$ in Eq. A-6.

The values of Δ and δ can be determined experimentally when the system is calibrated. The beam is then excited by a signal at the resonant frequency of the pickup cavities. The pickup cavities ($\lambda_q/4$ separated) are moved together along the beam and the standing-wave ratio of the output from the Magic Tee is observed. Let a, the standing-wave ratio, be

$$a = \frac{2 + (\Delta^2 + (1\mp r)^2\delta^2)^{1/2}}{2 - (\Delta^2 + (1\mp r)\delta^2)^{1/2}} \tag{42}$$

where the minus sign with r is for Eq. 40, and the plus sign is for Eq. 41. For the case of r = 0.5, α = 1, and a = 2 db, the error in the measurement of A_2/A_1 is not greater than 2 per cent in both cases. Since, in our measurements, the residual standing-wave ratio a was usually between 1.3 db and 2.0 db, the error introduced by this can be considered less than 2 per cent.

The third cause of error, the deviation of the distance between the two cavities from 1/4 plasma wavelength, has the same effect on the measurement of A_2/A_1 as the improper phase-shift adjustment. Usually, since the plasma wavelength λ_q can be measured with an accuracy of 0.5 mm, this cause of error is negligibly small compared with the other two.

Next, we consider the error caused by the variation of the beam current. During the measurement, after the selective beam coupler is properly adjusted, the beam current might change at the fixed-anode voltage. This change in the beam current causes a change in the plasma wavelength λ_q and in the characteristic impedance of the beam. The former effect is the same as the deviation of the distance between the two cavities from the 1/4 plasma wavelength, and the latter effect causes a change in the equivalent series resistance r of the first cavity. We can estimate these errors by formulas 40 and 41. We found that they are negligibly small for a 10 per cent variation in the beam current.

2. Error caused by calibration with imperfect white noise. When the coefficient of K_1/K_2 is calibrated with a noise which is not perfect white noise, but has some finite bandwidth, an error might be introduced in the measurement of A_2/A_1. Assuming that the bandwidth of the receiver is nearly equal to the bandwidth of the pickup cavities (which is the case with our measuring equipment), and the ratio of the bandwidth of the cavities to the bandwidth of the calibrating noise is γ, then the value of K_1/K_2 is given by

$$\frac{K_1}{K_2} = \frac{1 - \dfrac{1+3\gamma}{4(1+\gamma)(1+2\gamma)}\, r}{1 + \dfrac{1+3\gamma}{4(1+\gamma)(1+2\gamma)}\, r} \tag{43}$$

If the noise is perfectly white, the value of K_1/K_2 is given by setting $\gamma = 0$ in Eq. 43

$$\frac{K_1}{K_2} = \frac{1 - \dfrac{r}{4}}{1 + \dfrac{r}{4}} \tag{44}$$

For the cases $\gamma = 0.75$ (the noise bandwidth is 8 mc, the cavity bandwidths, 6 mc), and $r = 0.5$, the error is approximately 4 per cent.

3. Error from higher-order modes of the beam. The electron beam generally consists not only of the fundamental mode, but also of higher-order modes with small amplitudes, which thus far we have neglected. The noise parameters S and Π are defined under the assumption that only the fundamental mode plays the effective role in the noise figure of the beam. Such an assumption is usually valid because of the presence of small amplitudes from higher-order modes, and the weaker coupling to the rf structure of the beam tubes. Now, we want to investigate the error in the measurement of A_2/A_1 that arises from higher-order modes, and verify the fact that such a small amplitude from higher-order modes does not seriously affect the measured value of Π/S.

To make the problem simple, we assume that only one higher-order mode exists and the equivalent series resistance of the first cavity r for this mode is small enough to be neglected. Although the effect of the higher-order mode on the outputs of the selective coupler depends upon the phase relation between the fundamental and higher-order modes, the following equation can be obtained in the limiting case (the worst case of the phase relation).

$$\frac{\sum |I_{ta}|^2_{mean}}{\sum |I_{tb}|^2_{mean}} \approx \frac{K_1}{K_2} \frac{X_a + Y_a + \Delta Y_a \cos\theta}{X_b + Y_b + \Delta Y_b \cos\theta} \tag{45}$$

where

$$X_a = \left(1 - \frac{r}{2(1+a)} + \frac{r^2}{8(1+a)}\right) A_1 + \frac{r^2}{8(1+a)} A^2$$

$$X_b = \frac{r^2}{8(1+a)} A_1 + \left(1 + \frac{r}{2(1+a)} + \frac{r^2}{8(1+a)}\right) A_2$$

$$Y_a = \frac{\eta^2}{4}\left[P^2(1-r)^2 A'_1 + Q^2 A'_2\right]$$

$$Y_b = \frac{\eta^2}{4}\left[Q^2(1+r)^2 A'_1 + P^2 A'_2\right]$$

$$\Delta Y_a = \frac{\eta^2}{4}\left[2PQ(1-r)A'_{12}\right]$$

$$\Delta Y_b = \frac{\eta^2}{4}\left[2PQ(1+r)A'_{12}\right]$$

$$P = \sqrt{(1 - \sin\theta)^2 + \cos^2\theta} \qquad Q = \sqrt{(1 + \sin\theta)^2 + \cos^2\theta}$$

$$\theta = \beta'_q \Delta z = \frac{\pi}{2}\frac{\lambda_q}{\lambda'_q} \qquad \eta = \frac{Y'_o}{Y_o}\frac{M'}{M'}$$

and all primes indicate the parameters for the higher-order modes. Since in Eq. 45 Y_a, Y_b, ΔY_a, and ΔY_b become zero when the higher-order mode can be neglected, the effect of the higher-order mode on the measurement of A_2/A_1 can be calculated from this equation. As a numerical example, if we assume that $A_1' = A_2' = A_{12}'$, (the higher-order mode is not correlated and has a pure standing wave), and the higher-order mode is approximately 10 db less than the fundamental mode, including the coupling between the beam and cavity ($\eta^2 A_1'/A_1 = 0.1$), and $\lambda_q/\lambda_q' = 0.56$, $r = 0.5$, then the error can be calculated as 3 per cent for the case $A_2/A_1 = 0.6$, and 9 per cent for the case $A_2/A_1 = 1.0$ (no correlation).

4. Error in the Measurement of $\frac{\sum |I_{ta}|^2_{mean}}{\sum |I_{tb}|^2_{mean}}$. Since the calibration of the coefficient K_1/K_2 is done with the high-level signal and white noise of an amplitude that is sufficiently larger than the beam and thermal noises, the error arising from the fluctuations of the receiver and radiometer is negligibly small. But some error will be introduced by these factors in the measurement of the beam noise. With our system properly adjusted, an error of this kind in the measurement of $\Sigma |I_{ta}|^2_{mean}/\Sigma |I_{tb}|^2_{mean}$ was estimated as approximately 5 per cent.

However, we have to consider another source of error in the noise measurement. Sometimes, the outputs of the selective beam coupler increase linearly with the distance between the cathode and pickup cavities. We are not sure of the real reason for this at this stage; it may be attributable to the additional noise caused by the collision between electrons and gas molecules. The linearly increasing output of the selective beam coupler makes it difficult to determine exactly the mean value, $\Sigma |I_{ta}|^2_{mean}$ or $\Sigma |I_{tb}|^2_{mean}$. To eliminate uncertainty in the determination of the mean value, we measured two successive maxima and one minimum, or two successive minima and one maximum of the linearly increasing standing-wave pattern. From these data, we defined the ratio of $\frac{\sum |I_{ta}|^2_{mean}}{\sum |I_{tb}|^2_{mean}}$ at the nearest point to the cathode. (See Appendix IV.)

From the aforementioned calculations of the error, we computed the probable error in the measurement of A_2/A_1, and estimated it at from 7 to 10 per cent (depending upon the value of A_2/A_1 to be measured, and on other parameters) in almost all of our measurements. The coefficient of the second term of Eq. 39, however, is seriously affected by the value of A_2/A_1; and it might be very large, especially where A_2/A_1 approaches 1. In the other words, the percentage of error of II/S at the small correlation (II→0) will be largely affected by the error in the measurement of A_2/A_1. The estimated error for each measurement will be found in Tables II, III, V, VI, VII, VIII, and IX.

7.2 ERROR IN THE MEASUREMENT OF S

The error in the measurement of S consists of the error in the measurement of the beam-noise standing-wave ratio, ρ, and the error in the shot-noise calibration. Since the former is estimated at 4 per cent, and the latter at 6 per cent, the total probable error in the measurement of S is approximately 8 per cent.

VIII. CONCLUSION

We have described the measuring method of the noise parameters S and Π, by using a selective beam coupler, and the measured results of the two types of electron gun, the RCA low-noise gun and the parallel-flow gun. From the results the following conclusions can be drawn:

1. This measuring method can make it possible to measure the ratio of Π/S independently of S, and to improve the accuracy in Π/S-measurement, because no error is introduced in the S-measurement. This advantage is, also, very important, especially when it is desirable to measure the change of the noise parameters with the variation of other parameters.

2. Measured value of Π/S was of the order of $0.2 \sim 0.35$ in the space-charge-limited region, and almost zero in the temperature-limited region.

3. Π/S was slightly negative, of the order of -0.10 immediately after activation.

4. The measured values 2 and 3 agreed qualitatively with the results obtained by an independent method.[7, 8]

5. Although several measurements were made with changes in the electric-field distribution near the potential minimum, appreciable results could not be obtained. Further investigation is called for.

6. The errors in measurements of S and Π/S were discussed by taking account of the residual selectivity of the coupler, the effect of the pickup cavities upon the beam, the thermal noise from these cavities, and the higher-order modes. The error in the measurement of S was approximately 8 per cent, and that in the measurement of Π/S was approximately 0.04 in the absolute value of Π/S.

APPENDIX I

GENERALIZED EQUATIONS

We shall treat the general case of two nonidentical cavities and a detector circuit of finite bandwidth. The same notations as those given in the body of the report are used, except for the suffixes attached to the parameters. Suffixes 1 and 2 indicate the parameters of cavities 1 and 2.

The output currents I_{ta} and I_{tb} for cases a and b are given as (see Fig. 4):

$$I_{ta} = \sqrt{2Y_o}\, L_{2a}\, e^{-j\psi_a} \left\{ a_1\, e^{j\beta_q z_1} \times \left[M_1\, L_a \left(\frac{G_{L1}}{G_{t1}}\right) \frac{1}{1+jx_1} - M_2 \left(\frac{G_{L2}}{G_{t2}}\right) \frac{1}{1+jx_2} \left(1 - \frac{r}{1+jx_1}\right) \right] + a_2\, e^{-j\beta_q z_1} \times \left[M_1\, L_a \left(\frac{G_{L1}}{G_{t1}}\right) \frac{1}{1+jx_1} + M_2 \left(\frac{G_{L2}}{G_{t2}}\right) \frac{1}{1+jx_2} \left(1 + \frac{r}{1+jx_1}\right) \right] \right\} e^{-j\beta_e z_1}$$

for

$$L_{1a} = \frac{M_2}{M_1} \frac{\frac{G_{L2}}{G_{t2}}}{\frac{G_{L1}}{G_{t1}}} (1-r)\, L_{2a}, \quad \beta_q \Delta z = \pi/2, \quad \psi_a = \pi/2 + \beta_e \Delta z$$

and (A-1)

$$I_{tb} = \sqrt{2Y_o}\, L_{2b}\, e^{-j\psi_b} \left\{ a_1\, e^{j\beta_q z_1} \times \left[M_1\, L_b \left(\frac{G_{L1}}{G_{t1}}\right) \frac{1}{1+jx_1} + M_2 \left(\frac{G_{L2}}{G_{t2}}\right) \frac{1}{1+jx_2} \left(1 - \frac{r}{1+jx_1}\right) \right] + a_2\, e^{-j\beta_q z_1} \times \left[M_1\, L_b \left(\frac{G_{L1}}{G_{t1}}\right) \frac{1}{1+jx_1} - M_2 \left(\frac{G_{L2}}{G_{t2}}\right) \frac{1}{1+jx_2} \left(1 - \frac{r}{1+jx_1}\right) \right] \right\} e^{-j\beta_e z_1}$$

for

$$L_{1b} = \frac{M_2}{M_1} \frac{\frac{G_{L2}}{G_{t2}}}{\frac{G_{L1}}{G_{t2}}} (1+r)\, L_{2b}, \quad \beta_q \Delta z = \pi/2, \quad \psi_b = -\pi/2 + \beta_e \Delta z$$

If we assume that $F(\omega)$ is the frequency response of the receiving equipment, the integrated square currents $\Sigma|I_{ta}|^2$ and $\Sigma|I_{tb}|^2$ over the frequency range of the

measurements are

$$\sum |I_{ta}|^2 = \int_0^\infty |F(\omega)\, I_{ta}|^2 \, d\omega$$

$$\sum |I_{tb}|^2 = \int_0^\infty |F(\omega)\, I_{tb}|^2 \, d\omega \qquad \text{(A-2)}$$

A special case of these equations is treated in Appendix III.

In the measurement of S, the following equations are obtained for $\beta_q \Delta z = \pi$ and $\psi_c = \pi + \beta_e \Delta z$.

$$I_{tc} = \sqrt{2Y_o}\, e^{-j\psi_c} \left\{ M_1 L_c \left(\frac{G_{L1}}{G_{t1}}\right) \frac{1}{1 + jx_1} + M_2 \left(\frac{G_{L2}}{G_{t2}}\right) \frac{1}{1 + jx_2} \right\}$$

$$\times \left\{ a_1 e^{j\beta_q z_1} + a_2 e^{-j\beta_q z_1} \right\} e^{-j\beta_e z_1} \qquad \text{(A-3)}$$

$$\sum |I_{tc}|^2 = \int_0^\infty |F(\omega)|^2 = 2Y_o \left| M_1 L_c \left(\frac{G_{L1}}{G_{t1}}\right) \frac{1}{1 + jx_1} + M_2 \left(\frac{G_{L2}}{G_{t2}}\right) \frac{1}{1 + jx_2} \right|^2$$

$$\times \left\{ |a_1|^2 + |a_2|^2 + 2|a_1 a_2^*| \cos(2\beta_q z_1 - \phi_3) \right\}$$

Note that the frequency dependences of the cavity impedances and of the detector bandwidth do not affect the standing-wave measurements.

APPENDIX II

EFFECT OF THE DIFFERENCE BETWEEN THE Q-VALUES OF THE TWO CAVITIES

We shall investigate the effect upon the final results of the difference between the loaded Q's of the two pickup cavities. For ease in calculation, it is assumed that the resonant frequencies of both cavities are identical, $\omega_{o1} = \omega_{o2}$. This assumption facilitates practical operation, since it is easy to adjust the resonant frequencies of both cavities, but it is not as easy to adjust their Q's.

Setting $x_2 = \beta x_1$, in place of Eq. 31, from the generalized equation (A-1), we obtain directly

$$\sum |I_{ta}|^2_{mean} = 32\pi^2 (M_2 L_{2a})^2 \left(\frac{G_{L2}}{G_{t2}}\right)^2 Y_o \times \left[1 + \frac{q}{\beta(\beta+1)}\right] \left\{ \frac{p^2}{4(1+\beta)\left(1 + \frac{q}{\beta 1(\beta+1)}\right)} A_1 \right.$$

$$\left. + A_2 - \frac{1 - \frac{3}{2} r}{(1+\beta)\left(1 + \frac{q}{\beta(\beta+1)}\right)} \left(\frac{RT}{2\pi}\right) \right\}$$

$$\sum |I_{tb}|^2_{mean} = 32\pi^2 (M_2 L_{2b})^2 \left(\frac{G_{L2}}{G_{t2}}\right)^2 Y_o \times \left[1 + \frac{p}{\beta(\beta+1)}\right] \left\{ A_1 + \frac{q^2}{4(1+\beta)\left(1 + \frac{p}{\beta(\beta+1)}\right)} A_2 \right.$$

$$\left. + \frac{1 + \frac{3}{2} r}{(1+\beta)\, 1 + \frac{p}{\beta(\beta+1)}} \left(\frac{RT}{2\pi}\right) \right\} \qquad \text{(A-4)}$$

where $p = 1 - \beta + \beta r$, and $q = 1 - \beta - \beta r$.

APPENDIX III

EFFECT OF THE FREQUENCY RESPONSE OF THE RECEIVING RADIOMETER

We shall discuss the effect of the frequency response of the receiving equipment. It is assumed that $x_1 = x_2 (=x)$ and that the frequency response of the receiving equipment is $\frac{F}{1 + a^2 x^2}$. Then, from Eqs. A-1 and A-2, we obtain

$$\sum |I_{ta}|^2_{mean} =$$

$$32\pi^2 (M_2 L_{2a})^2 \left(\frac{G_{L2}}{G_{t2}}\right)^2 Y_o \frac{F}{1+a} \left\{ \frac{r^2}{8(1+a)} A_1 \right.$$

$$\left. + \left[1 - \frac{r}{2(1+a)} + \frac{r^2}{8(1+a)}\right] A_2 - \frac{1}{2}\left(1 - \frac{3}{2} r\right) \frac{2a+1}{a+1} \frac{kT}{2\pi} \right\} \qquad \text{(A-5)}$$

$$= K_1 \left\{ \frac{\frac{r^2}{8(1+a)}}{1 - \frac{r}{2(1+a)} + \frac{r^2}{8(1+a)}} A_1 + A_2 - \frac{1}{2}\left(1 - \frac{3}{2} r\right) \frac{2a+1}{(a+1)\left(1 - \frac{r}{2(1+a)} + \frac{r^2}{8(1+a)}\right)} \frac{kT}{2\pi} \right.$$

$$\sum |I_{tb}|^2_{mean} = 32\pi^2 (M_2 L_{2a})^2 \left(\frac{G_{L2}}{G_{t2}}\right)^2 Y_o \frac{F}{1+a} \left\{ \left(1 + \frac{r}{2(1+a)} + \frac{r^2}{8(1+a)}\right) A_1 \right.$$

$$\left. + \frac{r^2}{8(1+a)} A_2 + \frac{1}{2}\left(1 + \frac{3}{2} r\right) \frac{2a+1}{a+1} \frac{kT}{2\pi} \right\}$$

$$= K_2 \left\{ A_1 + \frac{\frac{r^2}{8(1+a)}}{\frac{r}{2(1+a)} + \frac{r^2}{8(1+a)}} A_2 \right. \tag{A-6}$$

$$\left. + \frac{1}{2}\left(1 + \frac{3}{2} r\right) \frac{2a+1}{(a+1)\left(1 + \frac{r}{2(1+a)} + \frac{r^2}{8(1+a)}\right)} \frac{kT}{2\pi} \right\}$$

$$\frac{K_2}{K_1} = \left(\frac{L_{2b}}{L_{2a}}\right)^2 \frac{1 + \frac{r}{2(1+a)} + \frac{r^2}{8(1+a)}}{1 - \frac{r}{2(1+a)} + \frac{r^2}{8(1+a)}} \tag{A-7}$$

where $\left(\frac{L_{2b}}{L_{2a}}\right)^2$ is equal to $\frac{1}{(1+r)^2}$ in actual measurement. From these equations, instead of from Eq. 32, the compensation factor caused by the finite selectivity of the selective beam coupler and the external thermal noise can be written

$$\left(\frac{A_2}{A_1}\right)_{ap} = \left(\frac{A_2}{A_1}\right)_{time} \frac{1 + \frac{\frac{r^2}{8(1+a)}}{1 - \frac{r}{2(1+a)} + \frac{r^2}{8(1+a)}} \frac{A_1}{A_2} - \frac{\frac{1}{2}\left(1 - \frac{3}{2} r\right) 2(a+1)}{(a+1)\left(1 - \frac{r}{2(1+a)} + \frac{r^2}{8(1+a)}\right)} \left(\frac{A_1}{A_2} - 1\right) \frac{\frac{kT}{k\pi}}{\overline{II}}}{1 + \frac{\frac{r^2}{8(1+a)}}{1 + \frac{r}{2(1+a)} + \frac{r^2}{8(1+a)}} \frac{A_2}{A_1} + \frac{\frac{1}{2}\left(1 + \frac{3}{2} r\right) 2(a+1)}{(a+1)\left(1 + \frac{r}{2(1+a)} + \frac{r^2}{8(1+a)}\right)} \left(1 - \frac{A_2}{A_1}\right) \frac{\frac{kT}{2\pi}}{\overline{II}}} \tag{A-8}$$

APPENDIX IV

EFFECT OF THE ADDITIONAL DISTRIBUTED NOISE

Sometimes we observed that the noise standing-wave pattern increased linearly with the distance between the cathode and the pickup cavities. In this case, we have to determine the actual standing-wave ratio and the mean value of the beam noise at any

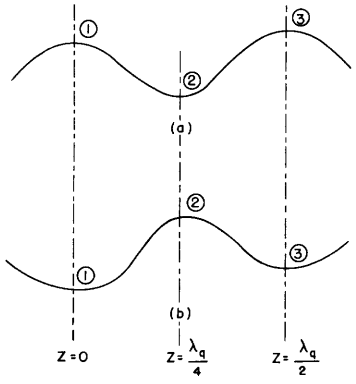

Fig. 23. Linearly growing "standing-wave pattern."

reference point. Although we do not know the reason for this increase in the beam noise, these values can be estimated by the assumption of an additional velocity fluctuation that is uniformly distributed along the beam. If we let the mean-square velocity fluctuation per unit length be v^2, the two outputs of the selective beam coupler that correspond to Eq. 22 can be given as

$$\sum |I_{ta}|^2 = C_1 \left\{ \frac{r^2}{8} (A_1 + A_1' 2\beta_q Z_1) + \left(1 - \frac{r}{2} + \frac{r^2}{8}\right)(A_2 + A_1' 2\beta_q Z_1) \right.$$
$$\left. - \frac{r}{2}\left(1 - \frac{r}{2}\right)\sqrt{A_1^2 + A_1'^2}\cos(2\beta_q Z_1 + \psi') + \frac{\pi}{2} A' \right\}$$
$$\sum |I_{tb}|^2 = C_2 \left\{ \left(1 + \frac{r}{2} + \frac{r^2}{8}\right)(A_1 + A_1' 2\beta_q Z_1) + \frac{r^2}{8}(A_2 + A_1' 2\beta_q Z_1) \right. \qquad \text{(A-9)}$$
$$\left. + \frac{r}{2}\left(1 + \frac{r}{2}\right)\sqrt{A_1^2 + A_1'^2}\cos(2\beta_q Z_1 + \psi') + \frac{\pi}{2} A' \right\}$$

where $A_1' = \dfrac{Y_o \bar{v}^2}{64\pi\beta_q}$, and Z_1 is the position of the first-cavity gap from the reference point. These equations show that the beam noise increases linearly with Z_1 because of the additional noise parameter A'.

In our measurements we could obtain two successive maxima and one minimum of the standing-wave pattern (Fig. 23a), or two successive minima and one maximum (Fig. 23b). Then the mean value at the reference point (Z = 0 of Fig. 23) can be calculated from the formula

$$\frac{a+1}{2} \frac{1}{1 + \dfrac{a(\beta-1)}{2 + a(3-\beta)}} \times \left(\begin{array}{l}\text{the value at the minimum point (2) for the} \\ \text{case of Fig. 23a.}\end{array}\right)$$

$$\frac{a+1}{2} \frac{1}{1 + \dfrac{a(\beta-1)}{2 + a(3-\beta)}} \times \left(\begin{array}{l}\text{the value at the minimum point (1) for the} \\ \text{case of Fig. 23b.}\end{array}\right)$$

where $\alpha(>1)$ is the ratio of two successive maxima or one minimum, and β is the ratio of the first maximum to the first minimum. If necessary, we can calculate the actual mean value of the beam noise at any point from the values of α and β.

Acknowledgment

This work has been done during the author's stay at the Research Laboratory of Electronics, Massachusetts Institute of Technology, on leave from the University of Tokyo, as a Fulbright Research Scholar from Japan. He is greatly indebted to Professor L. D. Smullin and to Professor H. A. Haus for their effective guidance and discussions. He is very grateful to the staff of the Tube Laboratory, Research Laboratory of Electronics, especially to Mr. A. Bers for helpful discussions and cooperation. Thanks are due Mr. C. Holly for his skilful assistance to the experiments. The author wishes also to express his gratitude to the Radio Corporation of America for supplying the low-noise guns for his experiments.

References

1. J. R. Pierce and W. E. Danielson, Minimum noise figure of traveling-wave tubes with uniform helices, J. Appl. Phys. 25, 1163-1165 (1954).
2. S. Bloom and R. W. Peter, A minimum noise figure for the traveling-wave tube, RCA Rev. 15, 252-267 (1954).
3. H. A. Haus and F. N. H. Robinson, The minimum noise figure of microwave beam amplifiers, Proc. IRE 43, 981-991 (1955).
4. A. E. Siegman, D. A. Watkins, and Hsung-Cheng Hsich, Density-function calculations of noise propagation on an accelerated multi-velocity electron beam, Informal Report, Stanford University, n.d.
5. C. C. Cutler and C. F. Quate, Experimental verification of space charge and transit time reduction of noise in electron beams, Phys. Rev. 80, 875-878 (1950).
6. L. D. Smullin and C. Fried, Microwave noise measurements on electron beams, Trans. IRE, vol. ED-1, no. 4, pp. 168-183 (Dec. 1954).
7. A. Bers, Experimental and theoretical aspects of noise in microwave tubes, S.M. Thesis, Department of Electrical Engineering, M.I.T., 1955.
8. T. J. Connor, Minimum noise figure of traveling-wave amplifier, S.M. Thesis, Department of Electrical Engineering, M.I.T., 1956.